

Fredholm–residue selection of the unsteady Kutta amplitude

Jiguang Yu^{a,1}, Louis Shuo Wang^{b,*,1}

^aCollege of Engineering, Boston University, Boston, 02215, MA, United States

^bDepartment of Mathematics, Northeastern University, Boston, 02115, MA, United States

ARTICLE INFO

Keywords:

unsteady Kutta selection
trailing-edge receptivity
viscous–inviscid matching
triple-deck theory
Fredholm compatibility
Wiener–Hopf method
wake-pole residue.
2020 MSC: 76G25, 76D10, 35Q35,
47A53, 35C15, 35C20

ABSTRACT

We give an operator-theoretic interpretation of unsteady Kutta selection in trailing-edge acoustic receptivity. The inviscid acoustic–wake problem leaves one outgoing wake amplitude undetermined. We show that, under explicit structural hypotheses, this amplitude is the same scalar obtained from three representations: cancellation of the inverse-square-root edge singularity, Fredholm compatibility of the viscous lower-deck problem, and the residue of the Kutta-normalized transform solution at the downstream wake pole: $A = -\frac{C_-^{(0)}}{C_-^{(KH)}} = -\frac{\langle \mathbf{F}_{\text{inc}}, \Psi^* \rangle}{\langle \mathbf{F}_{KH}, \Psi^* \rangle} = i \operatorname{Res}_{\alpha=\alpha_{KH}} \mathcal{M}(\alpha)$. The inner Fredholm–edge mechanism is verified exactly in a linear-shear lower-deck model, where the primal shear and adjoint velocity are Airy fields and the edge concomitant is nonzero outside a discrete resonance set.

1. Introduction and main identity

The unsteady Kutta condition is a singular selection principle at a sharp edge. In steady inviscid airfoil theory it fixes the circulation by removing the inverse-square-root velocity singularity at the trailing edge. In unsteady acoustic receptivity the situation is subtler: the outer acoustic–wake problem may admit an outgoing hydrodynamic wake mode, and the inviscid equations alone then leave one complex amplitude undetermined. This paper formulates that missing scalar as a Fredholm compatibility condition for the viscous lower-deck problem and identifies the same scalar with the pole residue of a Kutta-normalized transform solution. The structural hypotheses under which the identification holds are isolated and then verified in closed form for the canonical linear-shear model of the unsteady lower deck, for which the adjoint state is an Airy-derivative field and the edge concomitant is computable.

That a Kutta condition in unsteady flow need not coincide with its steady form, and that its applicability is itself a question, was surveyed in [12, 42, 44, 59, 3]. The vortex-sheet-from-an-edge problem and its sensitivity to the choice of edge condition were analyzed in [33, 46, 52, 23, 11, 10, 29, 36, 15] and the monograph of Howe [20, 28]. The viscous justification of the steady Kutta condition through triple-deck theory originates in [55, 39, 30, 40, 45, 41, 34, 22, 49]; the unsteady and oscillating-edge viscous structure was studied by Brown & Daniels [6], Daniels [13, 14], and Brown & Stewartson [7]. Boundary-layer receptivity to sound, in which an inviscid amplitude is fixed by an edge or solvability mechanism, is reviewed in [17, 57, 38, 18, 19, 37, 47, 58, 60, 51, 56]. The linearized unsteady lower deck about a uniform shear was solved exactly by Terent’ev in the vibrating-ribbon problem [43]; the worked example of Section 4 is its trailing-edge (plate–wake switching) analogue. The downstream/upstream classification of spatial poles we invoke is the Briggs–Bers criterion [5, 4, 31, 54, 21, 9, 1, 8, 27, 24, 53]. The transform analysis rests on the Wiener–Hopf technique [32, 50]; for finite-angle edges it is replaced by Mellin and functional-difference methods for wedges [25, 26, 15, 16, 48]. The contribution here is to tie the inner (viscous, Fredholm) and outer (transform, residue) selections together into a single conditional identity, with all structural hypotheses isolated, and to exhibit a model in which the inner hypotheses are theorems. The main contribution is not a full viscous proof for the physical trailing-edge base flow. Rather, it is a closed applied-mathematical selection mechanism: under explicitly stated structural hypotheses, the unsteady Kutta amplitude is the same scalar in three representations, namely the outer edge-regularity quotient, the lower-deck adjoint Fredholm quotient, and the downstream pole residue (Theorem 1.1, Figure 2). The inner part of this mechanism is then verified in closed form for the canonical linear-shear lower-deck model (Theorem 4.1).

*Corresponding author

✉ jyu678@bu.edu (J. Yu); wang.s41@northeastern.edu (L.S. Wang)

¹These authors contributed equally to this work as co-first authors.

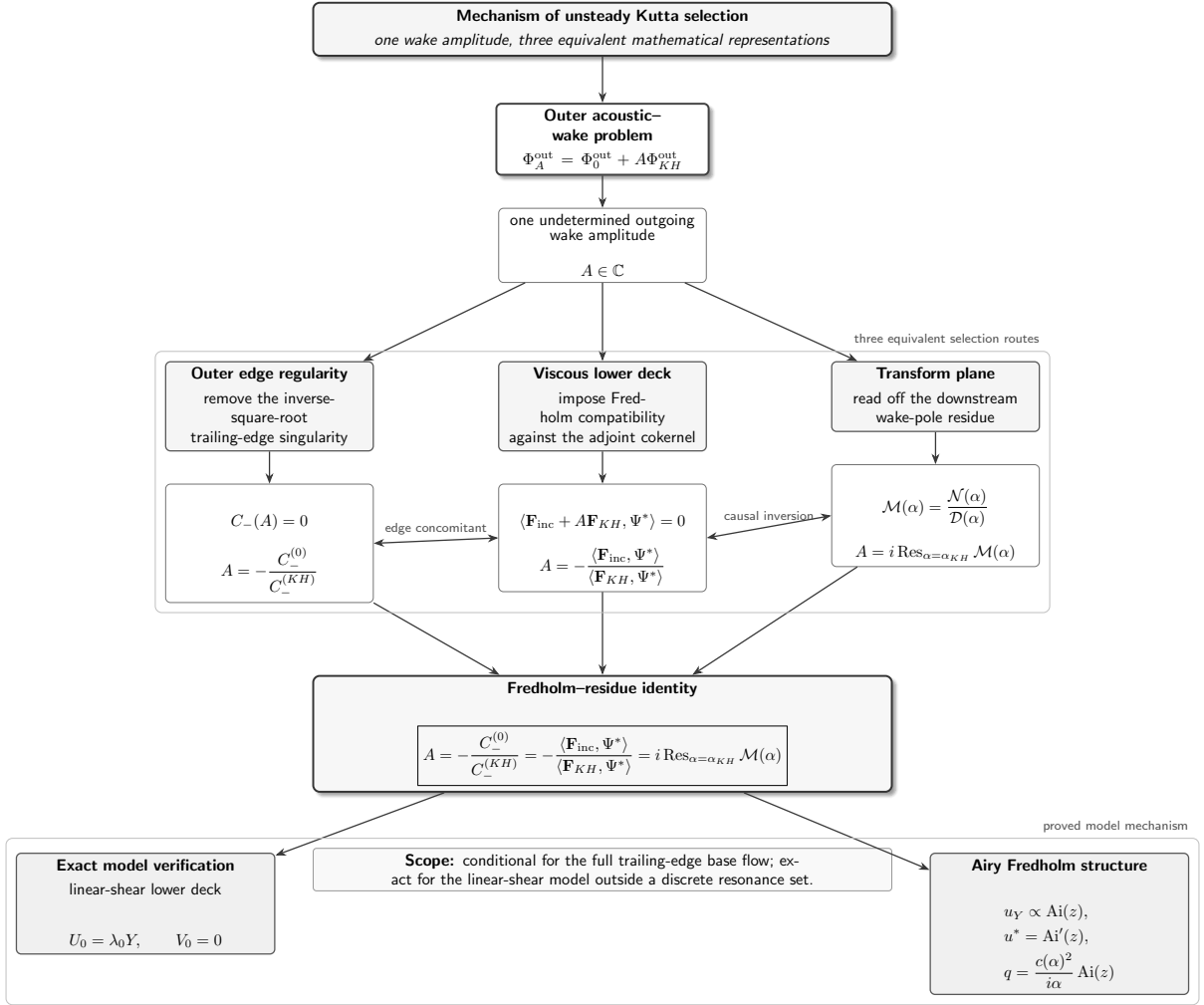


Figure 1: Mechanism of unsteady Kutta selection. The inviscid acoustic–wake problem leaves one outgoing wake amplitude A undetermined. The paper identifies three equivalent ways to select it: removal of the outer inverse-square-root edge singularity, Fredholm compatibility of the viscous lower-deck problem, and the residue of the Kutta-normalized transform solution at the downstream wake pole. The inner Fredholm–edge mechanism is verified exactly in the linear-shear lower-deck model, where the primal and adjoint fields are Airy fields.

Let

$$\Gamma_p = (-\infty, 0) \times \{0\}, \quad \Gamma_w = (0, \infty) \times \{0\}, \quad \Pi = \mathbb{R}^2 \setminus (\Gamma_p \cup \Gamma_w),$$

and let $O = (0, 0)$. We use $e^{-i\omega_{\text{phys}}t}$, set

$$M = \frac{U}{c} \in (0, 1), \quad \beta = (1 - M^2)^{1/2}, \quad k_0 = \frac{\omega_{\text{phys}}}{c}, \quad k = \frac{\omega_{\text{phys}}L}{U},$$

and write $\phi = \phi^{\text{inc}} + \phi^{\text{sc}}$. Two length scales are in play and must be kept distinct. The outer acoustic–wake problem (1.1)–(1.2) is posed on the hydrodynamic length $\ell_\omega = U/\omega_{\text{phys}}$, on which the Helmholtz number $k_0\ell_\omega = M$ is $\mathcal{O}(1)$ uniformly in the Reynolds number; the chord L enters only through Re and the triple-deck scalings of Section 3. All outer coordinates (x, y) below are measured on ℓ_ω ; the intermediate matching between this outer field and the lower

deck is part of the matching map \mathcal{M}_{in} introduced in (3.9) (for the hierarchy of unsteady regions see [6, 14]). In the outer region,

$$\mathcal{L}_{\text{out}}\phi = 0, \quad \mathcal{L}_{\text{out}} := \beta^2 \partial_x^2 + \partial_y^2 + 2iMk_0 \partial_x + k_0^2. \quad (1.1)$$

On Γ_p , $\gamma_p^\pm \partial_y \phi = 0$. On Γ_w , instead of imposing a degenerate equal-speed convected-sheet closure, we use an abstract inviscid-sheet transmission law

$$\mathcal{T}_{\text{sh}}(\omega_{\text{phys}}, \mathcal{G}) \begin{pmatrix} \gamma_w^+ \phi \\ \gamma_w^- \phi \\ \gamma_w^+ \partial_y \phi \\ \gamma_w^- \partial_y \phi \\ \eta \end{pmatrix} = 0, \quad x > 0.$$

Here $\eta(x)e^{-i\omega_{\text{phys}}t}$ is the sheet displacement and \mathcal{G} denotes the edge geometry, acoustic incidence, and base sheet data. The equal-speed relations

$$\partial_y \phi^\pm = (-i\omega_{\text{phys}} + U \partial_x) \eta, \quad (-i\omega_{\text{phys}} + U \partial_x)[\phi] = 0$$

are only a neutral limiting model; the downstream instability below belongs to the full operator \mathcal{T}_{sh} . We write the outgoing outer problem as

$$\mathcal{A}_{\text{out}}(\omega_{\text{phys}}, \mathcal{G})\Phi = \mathcal{F}_{\text{out}}^{\text{inc}}, \quad \Phi = (\phi, \eta). \quad (1.2)$$

For a homogeneous normal mode $\Phi(x, y) = e^{i\alpha x}(\varphi^+(y), \varphi^-(y), \eta_0)$, one obtains

$$(\varphi^\pm)'' - \mu(\alpha)^2 \varphi^\pm = 0, \quad \mu(\alpha)^2 = \beta^2 \alpha^2 + 2Mk_0 \alpha - k_0^2,$$

with the outgoing branch of μ . The sheet law reduces the normal-mode problem to

$$\mathcal{B}(\alpha; \omega_{\text{phys}}, \mathcal{G})\mathbf{a} = 0, \quad \mathcal{D}(\alpha; \omega_{\text{phys}}, \mathcal{G}) := \det \mathcal{B}(\alpha; \omega_{\text{phys}}, \mathcal{G}).$$

We assume a simple downstream wake pole

$$\mathcal{D}(\alpha_{KH}; \omega_{\text{phys}}, \mathcal{G}) = 0, \quad \partial_\alpha \mathcal{D}(\alpha_{KH}; \omega_{\text{phys}}, \mathcal{G}) \neq 0, \quad \Im \alpha_{KH} < 0.$$

With $e^{i\alpha x - i\omega_{\text{phys}}t}$, the last inequality corresponds to downstream spatial growth (a convective spatial instability; see the causal deformation of Section 5.3). The associated outgoing homogeneous field is $\Phi_{KH}^{\text{out}} = (\phi_{KH}^{\text{out}}, \eta_{KH})$, normalized once and for all by the wake functional ℓ_{KH} of (2.6), $\ell_{KH}(\Phi_{KH}^{\text{out}}) = 1$. The first structural hypothesis is the one-dimensional kernel $\ker \mathcal{A}_{\text{out}}^{\text{hom}} = \text{span}\{\Phi_{KH}^{\text{out}}\}$. Thus every outgoing forced outer field has the affine form

$$\Phi_A^{\text{out}} = \Phi_0^{\text{out}} + A \Phi_{KH}^{\text{out}}, \quad A \in \mathbb{C}. \quad (1.3)$$

The unknown scalar A is the receptivity amplitude. Near O , let (r, θ) denote polar coordinates after the local stretching $(x, y) \mapsto (x/\beta, y)$, $-\pi < \theta < \pi$. We assume the standard slit-plane edge pencil has first nonconstant indicial root $\lambda = 1/2$. Hence

$$\nabla \phi_A^{\text{out}} = C_-(A) r^{-1/2} \mathbf{V}_-(\theta) + \mathcal{O}(1), \quad \mathbf{V}_-(\theta) = \frac{1}{2} \Psi_-(\theta) \mathbf{e}_r + \Psi'_-(\theta) \mathbf{e}_\theta, \quad \Psi_-(\theta) = \sin \frac{\theta}{2}.$$

By linearity, $C_-(A) = C_-^{(0)} + AC_-^{(KH)}$. The outer regularity form of the Kutta condition is $C_-(A) = 0$. If $C_-^{(KH)} \neq 0$, this condition alone gives $A = -\frac{C_-^{(0)}}{C_-^{(KH)}}$. The central question is why this inviscid regularity condition is selected by the viscous trailing-edge structure. For the lower-deck scaling, set

$$Re = \frac{UL}{\nu}, \quad \varepsilon = Re^{-1/8}, \quad x = \varepsilon^3 L X, \quad y = \varepsilon^5 L Y, \quad T = \frac{Ut}{\varepsilon^2 L}.$$

Then

$$e^{-i\omega_{\text{phys}}t} = e^{-i\Omega T}, \quad \Omega = \frac{\omega_{\text{phys}}\varepsilon^2 L}{U} = \varepsilon^2 k = Re^{-1/4}k.$$

Thus the distinguished unsteady triple-deck regime is $\Omega = \mathcal{O}(1)$ with $k = \mathcal{O}(Re^{1/4})$. Linearization of the unsteady lower deck about a steady base state gives $\mathcal{L}_{\text{TD}}(\Omega)W = F$, where $W = (u, v, p, a)^\top$. The outer-to-inner matching data generated by (1.3) split as

$$F_{\text{match}}(A) = C_-(A)\mathbf{F}_{\text{sing}} + \mathbf{F}_{\text{inc}}(\Omega) + A\mathbf{F}_{KH}(\Omega), \quad \mathbf{F}_{\text{sing}} \in \mathcal{E}_{\text{edge}}, \quad \mathbf{F}_{\text{inc}} + A\mathbf{F}_{KH} \in \mathcal{H}_\sigma,$$

where $\mathcal{E}_{\text{edge}} = \text{span}\{r^{-1/2}\mathbf{V}_-\}$ is the singular edge-trace space; its lower-deck realization is an $|X|^{-1/2}$ line datum in the matching and pressure–displacement components, and as such it does not belong to the regular data space \mathcal{H}_σ (Theorem 3.1). Solvability in the bounded graph domain therefore requires

$$\Pi_{\text{sing}}F_{\text{match}}(A) = 0 \iff C_-(A) = 0.$$

The Fredholm realization is a closed densely defined operator $\mathcal{L}_{\text{TD}}(\Omega) : \mathcal{X}_\sigma \rightarrow \mathcal{H}_\sigma$ between the weighted spaces of Section 3.4, whose downstream weight is chosen so that the inner counterpart of the shed wake mode belongs to the domain (Remark 3.3). We assume

$$\text{ind } \mathcal{L}_{\text{TD}}(\Omega) = 0, \quad \ker \mathcal{L}_{\text{TD}}(\Omega)^* = \text{span}\{\Psi^*(\Omega)\}, \quad \langle \mathbf{F}_{KH}(\Omega), \Psi^*(\Omega) \rangle_{\mathcal{H}_\sigma} \neq 0.$$

The regular Fredholm condition is

$$\mathbf{F}_{\text{inc}}(\Omega) + A\mathbf{F}_{KH}(\Omega) \in \text{Ran } \mathcal{L}_{\text{TD}}(\Omega) \iff \langle \mathbf{F}_{\text{inc}}(\Omega) + A\mathbf{F}_{KH}(\Omega), \Psi^*(\Omega) \rangle_{\mathcal{H}_\sigma} = 0.$$

The edge trace and the regular Fredholm projection are linked by the consistency relation

$$\langle \mathbf{F}_{\text{inc}}(\Omega) + A\mathbf{F}_{KH}(\Omega), \Psi^*(\Omega) \rangle_{\mathcal{H}_\sigma} = \chi(\Omega)C_-(A), \quad \chi(\Omega) \neq 0. \quad (1.4)$$

This is not an independent hypothesis: in Section 3 (Proposition 3.5, Eq. (3.23)) it is derived from the Green identity of Appendix A together with the augmented solvability of (H3) below, with $\chi(\Omega) = -\kappa(\Omega)$; it thus reduces to nondegeneracy of the edge concomitant, $\kappa(\Omega) \neq 0$. Equivalently, $C_-(A) = 0$ iff $\mathbf{F}_{\text{inc}}(\Omega) + A\mathbf{F}_{KH}(\Omega) \in \text{Ran } \mathcal{L}_{\text{TD}}(\Omega)$. The same relation can be expressed through the finite edge concomitant

$$\mathcal{B}_{\text{edge}} : \mathcal{E}_{\text{edge}} \times \ker \mathcal{L}_{\text{TD}}(\Omega)^* \rightarrow \mathbb{C}, \quad \mathcal{B}_{\text{edge}}(C_-(A)r^{-1/2}\mathbf{V}_-, \Psi^*) = C_-(A)\kappa(\Omega),$$

with $\kappa(\Omega) = \mathcal{B}_{\text{edge}}(r^{-1/2}\mathbf{V}_-, \Psi^*(\Omega)) \neq 0$. Thus the singular edge cancellation and the Fredholm projection vanish for the same value of A . The transform formulation gives an independent representation of that same value. In the flat-plate case, the Kutta-normalized Wiener–Hopf solution is assumed meromorphic near α_{KH} , i.e., $\mathcal{M}(\alpha; \Omega, \mathcal{G}) = \frac{\mathcal{N}(\alpha; \Omega, \mathcal{G})}{D(\alpha; \Omega, \mathcal{G})}$.

With the wake normalization ℓ_{KH} of (2.6), the coefficient of the downstream wake mode is the residue at α_{KH} multiplied by the explicit contour-orientation factor i of (5.5). For finite-angle wedges with self-similar sheet data, the Fourier representation is replaced by a Mellin representation

$$\mathcal{M}_{\text{wedge}}(s; \Omega, \mathcal{G}) = \frac{\mathcal{N}_{\text{wedge}}(s; \Omega, \mathcal{G})}{D_{\text{wedge}}(s; \Omega, \mathcal{G})}, \quad A_{\text{rec}}^{\text{wedge}} = \text{Res}_{s=\alpha_{KH}} \mathcal{M}_{\text{wedge}}(s; \Omega, \mathcal{G}),$$

see Assumption B.1. We now state the main result (Figure 2).

Theorem 1.1 (Fredholm–residue identity for the unsteady Kutta amplitude). *Assume the following hypotheses:*

$$(H1) \quad \ker \mathcal{A}_{\text{out}}^{\text{hom}} = \text{span}\{\Phi_{KH}^{\text{out}}\}, \quad D(\alpha_{KH}; \omega_{\text{phys}}, \mathcal{G}) = 0, \quad D_\alpha(\alpha_{KH}; \omega_{\text{phys}}, \mathcal{G}) \neq 0, \quad \Im \alpha_{KH} < 0;$$

$$(H2) \quad \nabla \phi_A^{\text{out}} = C_-(A)r^{-1/2}\mathbf{V}_- + \mathcal{O}(1), \quad C_-(A) = C_-^{(0)} + AC_-^{(KH)}, \quad C_-^{(KH)} \neq 0;$$

(H3) $\mathcal{L}_{\text{TD}}(\Omega) : \mathcal{X}_\sigma \rightarrow \mathcal{H}_\sigma$ is Fredholm of index 0, $\ker \mathcal{L}_{\text{TD}}(\Omega)^* = \text{span}\{\Psi^*(\Omega)\}$, and for every $A \in \mathbb{C}$ the matching problem is solvable in the augmented class $\mathcal{D}_{\text{match}} = \mathcal{E}_{\text{edge}} \oplus \mathcal{H}_\sigma$;

(H4) $\kappa(\Omega) = \mathcal{B}_{\text{edge}}(r^{-1/2}\mathbf{V}_-, \Psi^*(\Omega)) \neq 0$ (with (H2)–(H3) this implies $\langle \mathbf{F}_{KH}, \Psi^* \rangle \neq 0$ and (1.4) with $\chi = -\kappa$);

(H5) $\mathcal{M}(\alpha; \Omega, \mathcal{G}) = \mathcal{N}(\alpha; \Omega, \mathcal{G})/\mathcal{D}(\alpha; \Omega, \mathcal{G})$ is the Kutta-normalized meromorphic transform response near α_{KH} .

Then bounded viscous–inviscid matching selects a unique amplitude

$$A_{\text{rec}}(\Omega, \mathcal{G}) = -\frac{C_-^{(0)}}{C_-^{(KH)}} = -\frac{\langle \mathbf{F}_{\text{inc}}(\Omega), \Psi^*(\Omega) \rangle_{\mathcal{H}_\sigma}}{\langle \mathbf{F}_{KH}(\Omega), \Psi^*(\Omega) \rangle_{\mathcal{H}_\sigma}} = i \text{Res}_{\alpha=\alpha_{KH}} \mathcal{M}(\alpha; \Omega, \mathcal{G}),$$

the last equality holding for the wake normalization $\ell_{KH}(\Phi_{KH}^{\text{out}}) = 1$ of (2.6). If α_{KH} is simple, then $A_{\text{rec}}(\Omega, \mathcal{G}) = \frac{i \mathcal{N}(\alpha_{KH}; \Omega, \mathcal{G})}{\partial_\alpha \mathcal{D}(\alpha_{KH}; \Omega, \mathcal{G})}$. Equivalently, $C_-(A) = 0$ iff $\Pi_{\text{sing}} F_{\text{match}}(A) = 0$ iff $\langle \mathbf{F}_{\text{inc}} + A\mathbf{F}_{KH}, \Psi^* \rangle_{\mathcal{H}_\sigma} = 0$ iff $\mathbf{F}_{\text{inc}} + A\mathbf{F}_{KH} \in \text{Ran } \mathcal{L}_{\text{TD}}(\Omega)$. For a finite-angle wedge satisfying the analogous Mellin hypotheses, including the self-similarity

$$\text{Assumption B.1, } A_{\text{rec}}^{\text{wedge}}(\Omega, \mathcal{G}) = -\frac{\langle \mathbf{F}_{\text{inc}}^{\text{wedge}}, \Psi_{\text{wedge}}^* \rangle_{\mathcal{H}_\sigma}}{\langle \mathbf{F}_{KH}^{\text{wedge}}, \Psi_{\text{wedge}}^* \rangle_{\mathcal{H}_\sigma}} = \text{Res}_{s=s_{KH}} \mathcal{M}_{\text{wedge}}(s; \Omega, \mathcal{G}).$$

Proof at the structural level. By (H1), every outgoing forced outer solution is $\Phi_A^{\text{out}} = \Phi_0^{\text{out}} + A\Phi_{KH}^{\text{out}}$. By (H2), its singular edge trace is $C_-(A)r^{-1/2}\mathbf{V}_-$. Since bounded lower-deck matching has data in \mathcal{H}_σ and the singular line datum is excluded from \mathcal{H}_σ by Lemma 3.1, the $\mathcal{E}_{\text{edge}}$ -component of $F_{\text{match}}(A)$ must vanish; hence $C_-(A) = 0$, which gives $A = -C_-^{(0)}/C_-^{(KH)}$. By (H3), the regular problem is solvable exactly when the Fredholm projection against Ψ^* vanishes. By (H3)–(H4) and Proposition 3.5, that Fredholm projection equals $-\kappa(\Omega)C_-(A)$, so the Fredholm-selected and Kutta-selected amplitudes coincide, giving the adjoint quotient. Finally, by (H5) and uniqueness of the Kutta-normalized outer field, the transform solution has the same amplitude; the causal inverse-transform deformation of Section 5.3 identifies this coefficient, in the normalization $\ell_{KH}(\Phi_{KH}^{\text{out}}) = 1$, with i times the residue at α_{KH} . The simple-pole formula is the Laurent coefficient of \mathcal{N}/\mathcal{D} . \square

The theorem is conditional in the following explicit places:

simple outgoing wake pole, edge indicial root $\lambda = 1/2$,

Fredholm lower-deck realization with augmented solvability,

nonzero edge concomitant, meromorphic Kutta-normalized transform.

Figure 1 shows the flowchart of our model. Sections 2 and 3 develop each object and prove the algebraic implications; Section 4 verifies the inner hypotheses (H3)–(H4) in closed form for the linear-shear model, where the adjoint state is an Airy-derivative field, the Wiener–Hopf kernel and wake pole are explicit, and $\kappa(\Omega) \neq 0$ off a discrete resonance set; Section 5 gives the transform representation and pole-residue formulae; Section 6 discusses scope and limitations; Appendix A derives the formal adjoint and edge concomitant; and Appendix B outlines the Mellin analogue for finite-angle wedges.

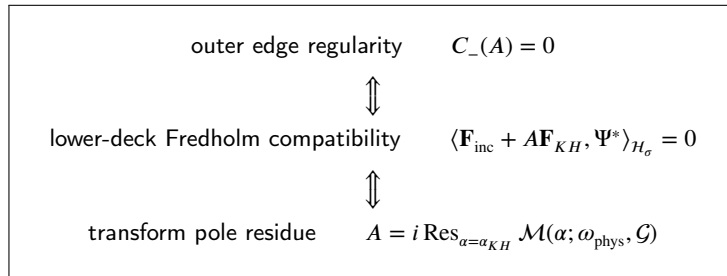


Figure 2: The selection mechanism of Theorem 1.1: the unsteady Kutta amplitude is the same scalar in three representations. The equivalences are Theorem 3.7 and Theorem 5.4; the nondegeneracies making them equivalences are (H2)–(H4).

2. Outer acoustic–wake problem and the edge obstruction

Let

$$\Gamma_p = (-\infty, 0) \times \{0\}, \quad \Gamma_w = (0, \infty) \times \{0\}, \quad \Pi = \mathbb{R}^2 \setminus (\Gamma_p \cup \Gamma_w).$$

The edge is $O = (0, 0)$. The incident acoustic field is denoted by ϕ^{inc} ; the total outer potential is

$$\phi = \phi^{\text{inc}} + \phi^{\text{sc}}, \quad \phi^\pm(x) = \lim_{y \rightarrow 0^\pm} \phi(x, y).$$

We use the convention $e^{-i\omega_{\text{phys}}t}$, and write

$$M = \frac{U}{c} \in (0, 1), \quad \beta = (1 - M^2)^{1/2}, \quad k_0 = \frac{\omega_{\text{phys}}}{c}, \quad k = \frac{\omega_{\text{phys}}L}{U}.$$

As stated in Section 1, the outer coordinates are measured on the hydrodynamic length $\ell_\omega = U/\omega_{\text{phys}}$, so that the outer problem is uniformly $\mathcal{O}(1)$ in Re throughout the distinguished regime (3.1). The physical configuration of the problem is illustrated in Figure 3, which consists of a semi-infinite rigid plate (Γ_p) and a downstream wake sheet (Γ_w).

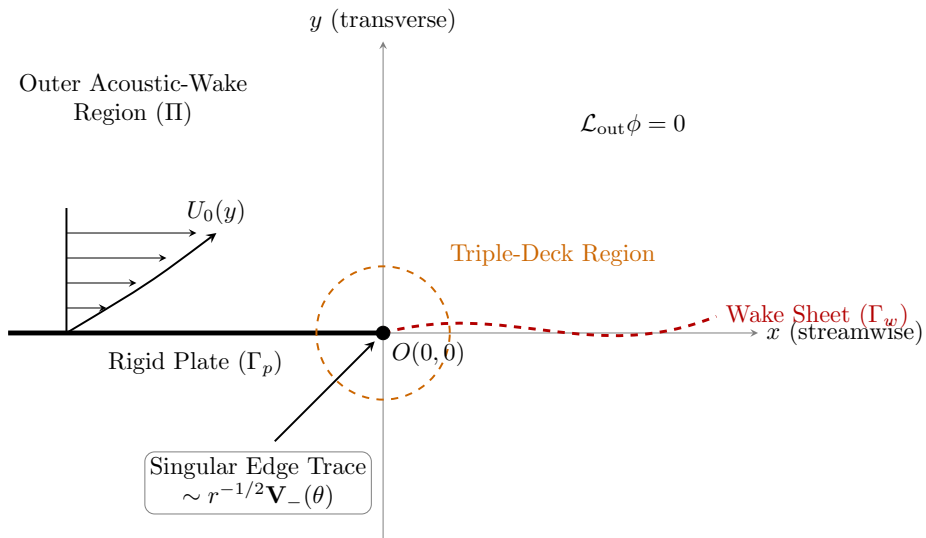


Figure 3: Schematic of the trailing-edge flow configuration. The physical domain includes the semi-infinite rigid plate Γ_p , the downstream wake sheet Γ_w , and the incoming boundary-layer velocity profile $U_0(y)$. The local triple-deck region and the outer acoustic-wake region around the trailing edge $O(0,0)$ are also highlighted.

2.1. Convected Helmholtz field and abstract sheet operator

In Π the scattered potential satisfies

$$\mathcal{L}_{\text{out}}\phi^{\text{sc}} = 0, \quad \mathcal{L}_{\text{out}} := \beta^2\partial_x^2 + \partial_y^2 + 2iMk_0\partial_x + k_0^2. \quad (2.1)$$

Equivalently, for the total potential,

$$\mathcal{L}_{\text{out}}\phi = 0, \quad \phi - \phi^{\text{inc}} \text{ outgoing.}$$

On the plate with $x < 0$, $\gamma_p^\pm(\partial_y\phi) = 0$, where $\gamma_p^\pm f = f(x, 0^\pm)$. On the wake we impose a linear inviscid-sheet transmission law

$$\mathcal{T}_{\text{sh}}(\omega_{\text{phys}}, \mathcal{G}) \begin{pmatrix} \gamma_w^+\phi \\ \gamma_w^-\phi \\ \gamma_w^+\partial_y\phi \\ \gamma_w^-\partial_y\phi \\ \eta \end{pmatrix} = 0, \quad x > 0, \quad (2.2)$$

where $\gamma_w^\pm f = f(x, 0^\pm)$, $\eta(x)e^{-i\omega_{\text{phys}}t}$ is the sheet displacement, and \mathcal{G} denotes the edge geometry, acoustic incidence, and base sheet data. Thus

$$\mathcal{G} = (M, \omega_{\text{phys}}, \text{edge angle, sheet strength, incidence data, } \dots).$$

The neutral equal-speed relations

$$\partial_y\phi^\pm = (-i\omega_{\text{phys}} + U\partial_x)\eta, \quad (-i\omega_{\text{phys}} + U\partial_x)[\phi] = 0, \quad [\phi] := \phi^+ - \phi^-,$$

are regarded only as a limiting convected-sheet model. The Kelvin–Helmholtz branch used below is attached to the full operator \mathcal{T}_{sh} , not to this degenerate equal- U limit [33, 10]. It is useful to collect the boundary data into $\mathbf{g}_w(\phi, \eta) := (\gamma_w^+\phi, \gamma_w^-\phi, \gamma_w^+\partial_y\phi, \gamma_w^-\partial_y\phi, \eta)^\top$. The outer problem is therefore

$$\mathcal{A}_{\text{out}}(\omega_{\text{phys}}, \mathcal{G}) \begin{pmatrix} \phi \\ \eta \end{pmatrix} = \begin{pmatrix} \mathcal{L}_{\text{out}}\phi \\ \gamma_p^\pm\partial_y\phi \\ \mathcal{T}_{\text{sh}}(\omega_{\text{phys}}, \mathcal{G})\mathbf{g}_w(\phi, \eta) \end{pmatrix} = \mathcal{F}_{\text{out}}^{\text{inc}}, \quad (2.3)$$

with outgoing radiation for the acoustic part and downstream causality for the hydrodynamic sheet modes. Here $\mathcal{F}_{\text{out}}^{\text{inc}}$ is the boundary forcing obtained after subtracting ϕ^{inc} . For later use we introduce the local trace spaces

$$\mathfrak{X}_{\text{out}} := H_{\text{loc}}^1(\Pi) \times H_{\text{loc}}^{1/2}(\Gamma_w), \quad \mathfrak{Y}_{\text{out}} := H_{\text{loc}}^{-1}(\Pi) \times H_{\text{loc}}^{-1/2}(\Gamma_p) \times \mathfrak{Z}_w,$$

and regard $\mathcal{A}_{\text{out}}(\omega_{\text{phys}}, \mathcal{G}) : \mathfrak{D}(\mathcal{A}_{\text{out}}) \subset \mathfrak{X}_{\text{out}} \rightarrow \mathfrak{Y}_{\text{out}}$ as the outgoing outer acoustic–wake operator. The precise Banach realization is not needed below; only the one-dimensional kernel and the local edge trace are used.

2.2. Assumed simple downstream wake pole

For a normal mode $(\phi, \eta)(x, y) = e^{i\alpha x}(\varphi^+(y), \varphi^-(y), \eta_0)$, (2.1) gives $(\varphi^\pm)'' - \mu(\alpha)^2\varphi^\pm = 0$ with $\mu(\alpha)^2 = \beta^2\alpha^2 + 2Mk_0\alpha - k_0^2$. The branch is fixed by the outgoing/decaying condition

$$\Re\mu(\alpha) > 0 \quad \text{on the physical inversion contour.}$$

Solving $\mu(\alpha)^2 = 0$ with $\beta^2 = (1 - M)(1 + M)$ gives $\alpha = k_0(-M \pm 1)/\beta^2$, i.e. the acoustic branch points

$$\alpha_+ = \frac{k_0}{1 + M}, \quad \alpha_- = -\frac{k_0}{1 - M}, \quad \text{i.e. } \alpha_\pm = \pm \frac{k_0}{1 \pm M}. \quad (2.4)$$

These are the downstream-propagating wavenumber $\omega_{\text{phys}}/(c + U)$ and the upstream wavenumber $-\omega_{\text{phys}}/(c - U)$. The sheet law (2.2) reduces the homogeneous normal-mode problem to a finite-dimensional algebraic system

$$B(\alpha; \omega_{\text{phys}}, \mathcal{G})\mathbf{a} = 0, \quad \mathbf{a} = (a_+, a_-, b_+, b_-, \eta_0)^\top.$$

Its dispersion determinant is $D(\alpha; \omega_{\text{phys}}, \mathcal{G}) := \det B(\alpha; \omega_{\text{phys}}, \mathcal{G})$, after removal of nonphysical normalization factors.

Assumption 2.1 (Simple downstream wake pole). There exists $\alpha_{KH} \in \mathbb{C}$ such that

$$\mathcal{D}(\alpha_{KH}; \omega_{\text{phys}}, \mathcal{G}) = 0, \quad \partial_{\alpha} \mathcal{D}(\alpha_{KH}; \omega_{\text{phys}}, \mathcal{G}) \neq 0, \quad \Im \alpha_{KH} < 0, \quad (2.5)$$

and $\ker \mathcal{B}(\alpha_{KH}; \omega_{\text{phys}}, \mathcal{G}) = \text{span}\{\mathbf{a}_{KH}\}$. The associated outgoing homogeneous field is denoted

$$\Phi_{KH}^{\text{out}} := (\phi_{KH}^{\text{out}}, \eta_{KH}), \quad \phi_{KH}^{\text{out}}(x, y) \sim e^{i\alpha_{KH}x} \varphi_{KH}(y), \quad x \rightarrow +\infty.$$

With the convention $e^{i\alpha x - i\omega_{\text{phys}}t}$, the inequality $\Im \alpha_{KH} < 0$ corresponds to downstream spatial growth—a convectively unstable wake mode in the Briggs–Bers sense [5, 4, 31]; the causal contour argument that justifies collecting it downstream is given in Section 5.3. The normalization is fixed once and for all by the explicit wake functional

$$\ell_{KH}(\Phi) := \lim_{x \rightarrow +\infty} e^{-i\alpha_{KH}x} \eta(x), \quad \ell_{KH}(\Phi_{KH}^{\text{out}}) = 1, \quad (2.6)$$

i.e. the normalized wake mode has unit displacement amplitude, $\eta_{KH}(x) = e^{i\alpha_{KH}x}$. We also record the abstract homogeneous assumption used below:

$$\ker \mathcal{A}_{\text{out}}^{\text{hom}}(\omega_{\text{phys}}, \mathcal{G}) = \text{span}\{\Phi_{KH}^{\text{out}}\}. \quad (2.7)$$

The analysis does not require an explicit formula for \mathcal{D} . It requires only (2.5) and (2.7).

2.3. One-dimensional kernel

Let

$$\Phi = (\phi, \eta), \quad \Phi_0^{\text{out}} = (\phi_0^{\text{out}}, \eta_0)$$

be one outgoing forced solution of (2.3). By (2.7), $\Phi_A^{\text{out}} = \Phi_0^{\text{out}} + A\Phi_{KH}^{\text{out}}$ for $A \in \mathbb{C}$, is the complete outgoing affine family with the same incident acoustic forcing.

Proposition 2.2 (One-dimensional kernel). *Assume (2.7). If $\mathcal{A}_{\text{out}} \Phi_0^{\text{out}} = \mathcal{F}_{\text{out}}^{\text{inc}}$, then $\mathcal{A}_{\text{out}} \Phi_A^{\text{out}} = \mathcal{F}_{\text{out}}^{\text{inc}}$ for any $A \in \mathbb{C}$. Conversely, if $\mathcal{A}_{\text{out}} \tilde{\Phi}^{\text{out}} = \mathcal{F}_{\text{out}}^{\text{inc}}$ and $\tilde{\Phi}^{\text{out}}$ satisfies the same outgoing convention, then $\tilde{\Phi}^{\text{out}} = \Phi_0^{\text{out}} + A\Phi_{KH}^{\text{out}}$ for a unique $A \in \mathbb{C}$.*

Proof. Linearity gives $\mathcal{A}_{\text{out}}(\Phi_0^{\text{out}} + A\Phi_{KH}^{\text{out}}) = \mathcal{F}_{\text{out}}^{\text{inc}} + A\mathcal{A}_{\text{out}}\Phi_{KH}^{\text{out}} = \mathcal{F}_{\text{out}}^{\text{inc}}$. If $\tilde{\Phi}^{\text{out}}$ is another outgoing solution, then $\tilde{\Phi}^{\text{out}} - \Phi_0^{\text{out}} \in \ker \mathcal{A}_{\text{out}}^{\text{hom}}$, hence $\tilde{\Phi}^{\text{out}} - \Phi_0^{\text{out}} = A\Phi_{KH}^{\text{out}}$. Uniqueness of A follows from $\Phi_{KH}^{\text{out}} \neq 0$. \square

Thus the outer inviscid problem fixes the acoustic field only modulo Φ_{KH}^{out} . The scalar $A = \ell_{KH}(\Phi_A^{\text{out}} - \Phi_0^{\text{out}})$ is the outer receptivity amplitude.

2.4. Local edge expansion and the coefficient $C_-(A)$

Let (r, θ) , $0 < r < r_0$, $-\pi < \theta < \pi$, denote polar coordinates after the local stretching

$$X_o = \frac{x}{\beta}, \quad Y_o = y;$$

the coefficients in the unstretched frame differ by explicit powers of β , immaterial to the affine structure in A used below. Near O , $\mathcal{L}_{\text{out}} = \beta^2 \partial_x^2 + \partial_y^2 + \text{lower-order terms}$, so after the stretching the principal symbol is $|\xi|^2 + |\zeta|^2$. Hence the indicial operator is the slit-plane Laplacian with the principal edge transmission constraints; the Kondrat'ev theory of corner asymptotics [25] applies. We assume the first nonconstant indicial root is the Neumann slit-plane root.

Assumption 2.3 (Edge indicial structure). The principal edge pencil $\mathfrak{P}(\lambda; \mathcal{G})$ has $\lambda_0 = 0$ and $\lambda_1 = \frac{1}{2}$, where λ_1 is simple modulo the constant mode and carries no logarithmic terms. The corresponding angular function may be chosen as $\Psi_-(\theta) = \sin \frac{\theta}{2}$ after the local elliptic stretching. The lower-order convective/acoustic terms and the sheet trace equations do not shift λ_1 ; they only determine higher coefficients and linear relations among the edge amplitudes.

For the principal slit problem,

$$\partial_\theta \Psi(\pm\pi) = 0, \quad \Psi'' + \lambda^2 \Psi = 0,$$

so the indicial roots are $\lambda_n = n/2$, with angular functions

$$\Psi_n(\theta) = \begin{cases} \sin \frac{n\theta}{2}, & n \text{ odd}, \\ \cos \frac{n\theta}{2}, & n \text{ even}, \end{cases}$$

the Neumann conditions at $\theta = \pm\pi$ selecting alternating parities. In particular the first nonconstant mode is $\Psi_1 = \Psi_- = \sin(\theta/2)$. The singular velocity profile associated with Ψ_- is

$$\mathbf{V}_-(\theta) = \frac{1}{2} \Psi_-(\theta) \mathbf{e}_r + \Psi'_-(\theta) \mathbf{e}_\theta, \quad \mathbf{e}_r = (\cos \theta, \sin \theta), \quad \mathbf{e}_\theta = (-\sin \theta, \cos \theta). \quad (2.8)$$

Equivalently,

$$\mathbf{V}_- \cdot \mathbf{e}_x = -\frac{1}{2} \sin \frac{\theta}{2}, \quad \mathbf{V}_- \cdot \mathbf{e}_y = \frac{1}{2} \cos \frac{\theta}{2}. \quad (2.9)$$

Thus

$$\mathbf{V}_- \cdot \mathbf{e}_x|_{\theta=\pi} = -\frac{1}{2}, \quad \mathbf{V}_- \cdot \mathbf{e}_x|_{\theta=-\pi} = +\frac{1}{2}, \quad \mathbf{V}_- \cdot \mathbf{e}_y|_{\theta=0} = \frac{1}{2}.$$

Define the edge coefficient $C_-(\Phi)$ by the asymptotic projection

$$C_-(\Phi) := \lim_{\rho \downarrow 0} \frac{\int_{-\pi}^{\pi} (\phi(\rho, \theta) - \bar{\phi}_\rho) \Psi_-(\theta) d\theta}{\rho^{1/2} \int_{-\pi}^{\pi} \Psi_-(\theta)^2 d\theta}, \quad \bar{\phi}_\rho = \frac{1}{2\pi} \int_{-\pi}^{\pi} \phi(\rho, \theta) d\theta. \quad (2.10)$$

Equivalently, C_- is the coefficient of the $r^{1/2} \Psi_-$ term in the Kondrat'ev expansion.

Proposition 2.4 (Edge expansion). *Assume Assumption 2.3. For each $A \in \mathbb{C}$,*

$$\phi_A^{\text{out}}(r, \theta) = \phi_e(A) + C_-(A) r^{1/2} \Psi_-(\theta) + r \Psi_0(A, \theta) + \mathcal{O}(r^{3/2})$$

in H^1 -conormal form as $r \downarrow 0$. Hence

$$\nabla \phi_A^{\text{out}}(r, \theta) = C_-(A) r^{-1/2} \mathbf{V}_-(\theta) + \mathbf{V}_0(A, \theta) + \mathcal{O}(r^{1/2}). \quad (2.11)$$

Moreover

$$C_-(A) = C_-^{(0)} + A C_-^{(KH)}, \quad C_-^{(0)} := C_-(\Phi_0^{\text{out}}), \quad C_-^{(KH)} := C_-(\Phi_{KH}^{\text{out}}). \quad (2.12)$$

Proof. The local elliptic pencil gives the conormal expansion

$$\phi_A^{\text{out}} = \sum_{\lambda \in \Lambda, \Re \lambda < 3/2} r^\lambda \Psi_\lambda(\theta) c_\lambda(A) + \mathcal{O}(r^{3/2}).$$

By Assumption 2.3, the only terms below $3/2$ relevant to the singular velocity are $\lambda = 0$, $\lambda = 1/2$, and $\lambda = 1$, with no logarithms. Thus the displayed expansion follows. Since $\nabla(r^{1/2} \Psi_-) = r^{-1/2} \left(\frac{1}{2} \Psi_- \mathbf{e}_r + \Psi'_- \mathbf{e}_\theta \right)$, (2.11) follows from (2.8). Finally, $\Phi_A^{\text{out}} = \Phi_0^{\text{out}} + A \Phi_{KH}^{\text{out}}$ and the projection (2.10) is linear; hence (2.12). \square

The singular pressure is obtained from the linearized Bernoulli relation

$$p[\phi] = -\rho_0(-i\omega_{\text{phys}} + U\partial_x)\phi.$$

Since $(-i\omega_{\text{phys}})r^{1/2}\Psi_- = \mathcal{O}(r^{1/2})$ and $\partial_x(r^{1/2}\Psi_-) = r^{-1/2}\mathbf{V}_- \cdot \mathbf{e}_x$,

$$p[\phi_A^{\text{out}}] = -\rho_0 U C_-(A) r^{-1/2} \mathbf{V}_-(\theta) \cdot \mathbf{e}_x + \mathcal{O}(1). \quad (2.13)$$

Thus the same scalar $C_-(A)$ controls the inverse-square-root velocity singularity and the leading pressure singularity. We introduce the singular edge trace space $\mathcal{E}_{\text{edge}} := \text{span}\{r^{-1/2}\mathbf{V}_-(\theta)\}$, and the regular edge data space $\mathcal{R}_{\text{edge}}$ by

$$\nabla\phi_A^{\text{out}} = C_-(A) r^{-1/2} \mathbf{V}_- + \mathcal{R}_A, \quad \mathcal{R}_A \in \mathcal{R}_{\text{edge}}.$$

Hence $\text{Tr}_{\text{sing}} \nabla\phi_A^{\text{out}} = C_-(A) r^{-1/2} \mathbf{V}_- \in \mathcal{E}_{\text{edge}}$. On the lower-deck scale $r = \varepsilon^3 L (X^2 + \varepsilon^4 Y^2)^{1/2}$, the trace of $\mathcal{E}_{\text{edge}}$ on the matching components is an $|X|^{-1/2}$ -profile line datum.

2.5. Kutta regularity as $C_-(A) = 0$

The outer regularity form of the Kutta condition is the annihilation of the singular edge trace:

$$\text{Tr}_{\text{sing}} \nabla\phi_A^{\text{out}} = 0 \iff C_-(A) = 0. \quad (2.14)$$

By (2.12),

$$A_{\text{Kutta}}^{\text{out}} = -\frac{C_-^{(0)}}{C_-^{(KH)}}, \quad C_-^{(KH)} \neq 0. \quad (2.15)$$

Lemma 2.5 (Uniqueness of the Kutta-normalized outer field). *Assume (2.7), Assumption 2.3, and $C_-^{(KH)} \neq 0$. Then there exists a unique $A \in \mathbb{C}$ such that Φ_A^{out} satisfies (2.14). It is given by (2.15). If $\tilde{\Phi}^{\text{out}}$ is any outgoing solution with the same incident forcing and $C_-(\tilde{\Phi}^{\text{out}}) = 0$, then $\tilde{\Phi}^{\text{out}} = \Phi_{A_{\text{Kutta}}^{\text{out}}}^{\text{out}}$.*

Proof. Every outgoing solution is Φ_A^{out} by Proposition 2.2. The Kutta condition is $C_-^{(0)} + AC_-^{(KH)} = 0$. Since $C_-^{(KH)} \neq 0$, the solution is unique and equals (2.15). \square

Equivalently, $\mathfrak{K} : \Phi_A^{\text{out}} \mapsto C_-(A)$ is a nontrivial linear functional on the one-dimensional kernel. The outer Kutta quotient is therefore $A_{\text{Kutta}}^{\text{out}} = -\frac{\mathfrak{K}(\Phi_0^{\text{out}})}{\mathfrak{K}(\Phi_{KH}^{\text{out}})}$. At this stage (2.14) is only an outer regularity condition. The viscous lower-deck analysis will identify it with a Fredholm compatibility condition:

$$C_-(A) = 0 \iff \mathbf{F}_{\text{inc}} + A\mathbf{F}_{KH} \in \text{Ran } \mathcal{L}_{\text{TD}}(\Omega) \iff \langle \mathbf{F}_{\text{inc}} + A\mathbf{F}_{KH}, \Psi^* \rangle_{\mathcal{H}} = 0.$$

Thus the scalar obstruction passed from the outer problem to the inner problem is precisely $C_-(A) = C_-^{(0)} + AC_-^{(KH)}$.

3. Unsteady lower deck and Fredholm Kutta selection

The outer field of Section 2 has

$$\nabla\phi_A^{\text{out}} = C_-(A) r^{-1/2} \mathbf{V}_- + \mathcal{R}_A, \quad C_-(A) = C_-^{(0)} + AC_-^{(KH)}.$$

We now derive the scalar condition selecting A from the viscous trailing-edge region. The viscous structure is the unsteady triple deck [39, 30, 40, 41].

3.1. Triple-deck scaling and distinguished frequency

Let

$$Re = \frac{UL}{\nu}, \quad \varepsilon = Re^{-1/8}, \quad x = \varepsilon^3 L X, \quad y = \varepsilon^5 L Y.$$

The main-deck thickness is $\mathcal{O}(\varepsilon^4 L)$; hence the lower-deck shear speed at $y = \mathcal{O}(\varepsilon^5 L)$ is

$$U_{LD} = \mathcal{O}(\varepsilon U), \quad \ell_{LD} = \mathcal{O}(\varepsilon^3 L), \quad t_{LD} = \frac{\ell_{LD}}{U_{LD}} = \frac{\varepsilon^2 L}{U}.$$

Thus

$$T = \frac{t}{t_{LD}} = \frac{Ut}{\varepsilon^2 L}, \quad e^{-i\omega_{\text{phys}} t} = e^{-i\Omega T}, \quad \Omega = \omega_{\text{phys}} t_{LD} = \frac{\omega_{\text{phys}} \varepsilon^2 L}{U}.$$

With $k = \omega_{\text{phys}} L/U$, $\Omega = \varepsilon^2 k = Re^{-1/4} k$. The distinguished unsteady lower-deck regime is

$$\Omega = \mathcal{O}(1), \quad k = \mathcal{O}(\varepsilon^{-2}) = \mathcal{O}(Re^{1/4}). \quad (3.1)$$

Use the lower-deck scales

$$u_{\text{phys}} = \varepsilon U U(X, Y, T), \quad v_{\text{phys}} = \varepsilon^3 U V(X, Y, T), \quad p_{\text{phys}} = \rho_0 \varepsilon^2 U^2 P(X, T).$$

Then the leading lower-deck equations are $U_X + V_Y = 0$ and $U_T + UU_X + VU_Y = -P_X + U_{YY}$.

3.2. Symmetry components and the two-sided wake

Downstream of the edge the deck occupies $Y \in \mathbb{R}$: the trailing-edge lower deck consists of two wall layers for $X < 0$, $\pm Y > 0$, merging into a two-sided wake layer for $X > 0$, with a smooth symmetric steady base state

$$U_0(X, -Y) = U_0(X, Y), \quad V_0(X, -Y) = -V_0(X, Y), \quad U_{0Y}(X, 0) = 0 \quad (X > 0),$$

cf. [39, 30, 22]. Unsteady perturbations carry, in addition to (u, v, p, a^\pm) , a wake-centerline displacement $h(X)e^{-i\Omega T}$, with linearized centerline conditions for $X > 0$

$$[u] = 0, \quad [u_Y] = 0, \quad v(X, 0^\pm) = (-i\Omega + U_c(X)\partial_X)h, \quad U_c(X) := U_0(X, 0), \quad (3.2)$$

where $[\cdot]$ denotes the jump across $Y = 0$ (the base smoothness $U_{0Y}(X, 0) = 0$ removes base-shear jump terms). Because the base state is symmetric, the linearized problem decomposes into a symmetric component (u even, v odd in Y , $h = 0$) and an antisymmetric component (u odd, v even, $h \neq 0$), each with its own pressure–displacement interaction map. On the half-plane $Y > 0$ these reduce to

$$\text{(both components)} \quad u = v = 0 \quad (X < 0, Y = 0^+); \quad (3.3)$$

$$\text{(symmetric)} \quad v = 0, \quad u_Y = 0 \quad (X > 0, Y = 0^+); \quad (3.4)$$

$$\text{(antisymmetric)} \quad u = 0, \quad v = (-i\Omega + U_c \partial_X)h \quad (X > 0, Y = 0^+). \quad (3.5)$$

The Kelvin–Helmholtz wake mode and its matching data are antisymmetric (the edge angular function $\sin(\theta/2)$ is odd); incident acoustic data generically force both components. All structural statements of this section (weighted realization, Fredholm hypothesis, adjoint, edge concomitant, and the selection Theorem 3.7) are formulated componentwise: $\mathcal{L}_{\text{TD}}(\Omega)$ denotes the linearized operator of either component on $Y > 0$, with the corresponding half-plane conditions and interaction law. For notational ease the displayed formulas below are written for the symmetric component (3.4), for which the worked example of Section 4 is carried out in closed form; the antisymmetric component differs only in the wake-side boundary block and in the explicit wake impedance, and is discussed in Remark 4.7. The upper matching condition is

$$U(X, Y, T) = \lambda_0 Y + \Delta(X, T) + o(1), \quad Y \rightarrow +\infty, \quad \lambda_0 > 0.$$

For the flat-plate subsonic upper-deck map of the relevant component,

$$P = \mathcal{K}[\Delta], \quad \mathcal{K} = H\partial_X, \quad \widehat{\mathcal{K}}a(\alpha) = |\alpha|\widehat{a}(\alpha), \quad (3.6)$$

where H is the Hilbert transform. For wedge geometries \mathcal{K} is replaced by the corresponding wedge pressure–displacement operator. Let $(U_0, V_0, P_0, \Delta_0)$ be a steady lower-deck solution:

$$\begin{aligned} U_{0X} + V_{0Y} &= 0, & U_0U_{0X} + V_0U_{0Y} &= -P_{0X} + U_{0YY}, \\ U_0 &\sim \lambda_0 Y + \Delta_0(X) \quad (Y \rightarrow \infty), & P_0 &= \mathcal{K}[\Delta_0], \end{aligned}$$

with (3.3)–(3.4). In particular,

$$U_{0X} + V_{0Y} = 0, \quad V_0|_{X>0, Y=0} = 0. \quad (3.7)$$

3.3. Linearized unsteady lower-deck operator

Set

$$U = U_0 + ue^{-i\Omega T}, \quad V = V_0 + ve^{-i\Omega T}, \quad P = P_0 + pe^{-i\Omega T}, \quad \Delta = \Delta_0 + ae^{-i\Omega T}.$$

The linearized system is

$$\begin{aligned} u_X + v_Y &= f_0, \\ -i\Omega u + U_0u_X + V_0u_Y + U_{0X}u + U_{0Y}v + p_X - u_{YY} &= f_1, \\ u(X, Y) - a(X) &\rightarrow f_\infty(X) \quad (Y \rightarrow \infty), \\ p - \mathcal{K}[a] &= f_K. \end{aligned} \quad (3.8)$$

The homogeneous boundary conditions are (3.3)–(3.4). Write $W = (u, v, p, a)^\top$ and $F = (f_0, f_1, f_\infty, f_K)^\top$. Then (3.8) with (3.3)–(3.4) defines $\mathcal{L}_{\text{TD}}(\Omega)W = F$. The outer-to-inner matching map is denoted $\mathcal{M}_{\text{in}} : \Phi^{\text{out}} \mapsto F_{\text{match}}$. Linearity of matching gives

$$F_{\text{match}}(A) = \mathcal{M}_{\text{in}}[\Phi_A^{\text{out}}] = \mathbf{F}_{\text{inc}}(\Omega) + A\mathbf{F}_{KH}(\Omega) + C_-(A)\mathbf{F}_{\text{sing}}(\Omega), \quad (3.9)$$

where

$$\mathbf{F}_{\text{inc}} := \mathcal{M}_{\text{in}}[\Phi_0^{\text{out}}]_{\text{reg}}, \quad \mathbf{F}_{KH} := \mathcal{M}_{\text{in}}[\Phi_{KH}^{\text{out}}]_{\text{reg}},$$

the subscript denoting the part of the matching data remaining after the singular edge trace is split off. The singular datum is generated by $\nabla\phi_A^{\text{out}} = C_-(A)r^{-1/2}\mathbf{V}_- + \mathcal{R}_A$. Since $r = \varepsilon^3 L(X^2 + \varepsilon^4 Y^2)^{1/2}$, the singular trace enters the lower deck, at leading order, as the line datum

$$\mathbf{F}_{\text{sing}} = (0, 0, g_\infty^\#, g_K^\#), \quad g_\infty^\#(X) = c_\infty^\pm |X|^{-1/2}, \quad g_K^\#(X) = c_K^\pm |X|^{-1/2} \quad (\pm X > 0), \quad (3.10)$$

with the explicit constants

$$c_\infty^+ = 0, \quad c_\infty^- = \mp \frac{1}{2} \quad (\theta = \pm\pi), \quad c_K^+ = 0, \quad c_K^- = \pm \frac{1}{2} \quad (\theta = \pm\pi), \quad (3.11)$$

read off from (2.9) and (2.13) (slip and pressure traces upstream; on the wake side $\theta = 0$ the streamwise trace of \mathbf{V}_- vanishes and the singular content is carried by the transverse/displacement trace, which enters the antisymmetric component analogously). The normalization of c_∞^\pm, c_K^\pm is fixed once by the matching map and plays no role beyond the linearity $\mathbf{F}_{\text{sing}} \mapsto C_-(A)\mathbf{F}_{\text{sing}}$. The regular lower-deck problem therefore reads

$$\mathcal{L}_{\text{TD}}(\Omega)W = \mathbf{F}_{\text{inc}}(\Omega) + A\mathbf{F}_{KH}(\Omega), \quad (3.12)$$

provided $C_-(A) = 0$. The role of the next subsections is to show that this condition is also forced by Fredholm solvability. The formal L^2 -adjoint is obtained from the bilinear pairing $\iint_{\mathbb{R} \times \mathbb{R}_+} \{u^* R_1 + q R_0\} dX dY$, where

$$R_0 = u_X + v_Y, \quad R_1 = -i\Omega u + U_0u_X + V_0u_Y + U_{0X}u + U_{0Y}v + p_X - u_{YY}.$$

Using (3.7), the adjoint bulk equations are

$$-i\Omega u^* - U_0 u_X^* - V_0 u_Y^* + U_{0X} u^* - u_{YY}^* - q_X = 0, \quad q_Y = U_{0Y} u^*; \quad (3.13)$$

the full derivation, with the line and edge terms, is in Appendix A. The Lagrange concomitant is

$$J^X = qu + U_0 u^* u + u^* p, \quad J^Y = qv + V_0 u^* u - (u^* u_Y - u_Y^* u). \quad (3.14)$$

The transposed wall/wake conditions are

$$u^* = 0 \quad (X < 0, Y = 0), \quad u_Y^* = 0 \quad (X > 0, Y = 0),$$

together with decay at $Y = \infty$. Treating $p = \mathcal{K}[a]$ and $u(\cdot, \infty) = a$ with line multipliers gives

$$b = \bar{U}_X^*, \quad \mu = \mathcal{K}[\bar{U}_X^*] = H[\bar{U}_{XX}^*], \quad \bar{U}^*(X) := \int_0^\infty u^*(X, Y) dY. \quad (3.15)$$

3.4. Weighted spaces and Fredholm hypothesis

Let $\langle X \rangle = (1 + X^2)^{1/2}$ and define, for $\sigma = (\sigma_-, \vartheta)$ with $\sigma_- > 0$ and $\vartheta > 0$,

$$w_\sigma(X) = \begin{cases} \langle X \rangle^{\sigma_-}, & X < 0, \\ e^{-\vartheta X}, & X > 0, \end{cases} \quad (3.16)$$

with $\vartheta > |\Im \alpha_{KH}^{\text{in}}|$, where α_{KH}^{in} is the inner wavenumber of the shed wake mode. Thus algebraic decay is demanded upstream, while the exponential downstream weight admits the spatially growing or neutral wake response into the function class; this choice is what produces the one-dimensional kernel and cokernel below (Remark 3.3). For a scalar field g , set $\|g\|_{L_\sigma^2}^2 = \iint_{\mathbb{R} \times \mathbb{R}_+} |w_\sigma(X)g(X, Y)|^2 dX dY$, and analogously for line functions. Define the anisotropic model domain

$$\begin{aligned} \mathcal{X}_\sigma := \{W = (u, v, p, a) : u, u_X, u_{YY}, v, v_Y \in L_\sigma^2, \\ p, p_X \in L_\sigma^2(\mathbb{R}), \quad a, \mathcal{K}a \in H_\sigma^1(\mathbb{R}), \\ u - a \rightarrow 0 \quad (Y \rightarrow \infty), \quad (3.3), (3.4) \text{ hold in trace sense}\}, \end{aligned}$$

a Banach space with its natural norm. The data space is

$$\mathcal{H}_\sigma := L_\sigma^2(\Pi) \times L_\sigma^2(\Pi) \times H_\sigma^{1/2}(\mathbb{R}) \times H_\sigma^{-1/2}(\mathbb{R}). \quad (3.17)$$

The realization of $\mathcal{L}_{\text{TD}}(\Omega)$ is the bounded operator $\mathcal{L}_{\text{TD}}(\Omega) : \mathcal{X}_\sigma \rightarrow \mathcal{H}_\sigma$ between these Banach spaces; the adjoint $\mathcal{L}_{\text{TD}}(\Omega)^*$ acts on the dual weight class (in particular, adjoint states decay downstream faster than $e^{-\vartheta X}$, localizing the adjoint near the edge and upstream, as in receptivity theory [17]).

Lemma 3.1 (Trace-level exclusion of the singular datum). $\mathbf{F}_{\text{sing}} \notin \mathcal{H}_\sigma$; more precisely the line profiles $g_\infty^\sharp, g_K^\sharp \sim c^\pm |X|^{-1/2}$ of (3.10) satisfy $|X|^{-1/2} \notin L_{\text{loc}}^2(\mathbb{R}) \supset H_{\text{loc}}^{1/2}(\mathbb{R})$, hence $\mathcal{E}_{\text{edge}} \cap \mathcal{H}_\sigma = \{0\}$, and $\mathcal{D}_{\text{match}} := \mathcal{E}_{\text{edge}} \oplus \mathcal{H}_\sigma$ is a well-defined direct sum, and the projection Π_{sing} onto the $\mathcal{E}_{\text{edge}}$ -component is well defined.

Proof. $\int_0^1 |X|^{-1} dX = \infty$, so $|X|^{-1/2}$ is not locally square integrable on the line; a fortiori it does not belong to $H_\sigma^{1/2}(\mathbb{R})$ or $H^{-1/2} \cap L^2$ -regular classes used in (3.17). (Note that the corresponding bulk field $r^{-1/2} \mathbf{V}_-$ is locally square integrable in two dimensions; the exclusion is genuinely a trace-level statement, which is why \mathbf{F}_{sing} is recorded as a line datum in (3.10).) Since $\mathbf{F}_{\text{sing}} \neq 0$ has zero bulk components and non- \mathcal{H}_σ line components, $\mathcal{E}_{\text{edge}} \cap \mathcal{H}_\sigma = \{0\}$. \square

Hypothesis 3.2 (Fredholm lower-deck structure with augmented solvability). For each fixed Ω in (3.1):

1. $\mathcal{L}_{\text{TD}}(\Omega) : \mathcal{X}_\sigma \rightarrow \mathcal{H}_\sigma$ is Fredholm of index zero,

$$\text{ind } \mathcal{L}_{\text{TD}}(\Omega) = 0, \quad (3.18)$$

and

$$\ker \mathcal{L}_{\text{TD}}(\Omega)^* = \text{span}\{\Psi^*(\Omega)\}, \quad \Psi^* = (u^*, q, b, \mu); \quad (3.19)$$

2. (augmented solvability) for every $A \in \mathbb{C}$ there exists a field W_A in the augmented graph class associated with $\mathcal{D}_{\text{match}} = \mathcal{E}_{\text{edge}} \oplus \mathcal{H}_\sigma$ such that $\mathcal{L}_{\text{TD}}(\Omega)W_A = F_{\text{match}}(A)$, and the Green identity (A.1) holds for the pair (W_A, Ψ^*) with finite edge concomitant.

Part (ii) is the precise statement needed to read the compatibility relation below as an identity in A ; it is not implied by part (i), and in the abstract setting it is part of limitation (i) of Section 6. In the linear-shear model of Section 4 it holds automatically: the Wiener–Hopf construction produces solutions for both the Kutta and the non-Kutta edge normalizations, the latter realizing exactly the singular class $\mathcal{E}_{\text{edge}}$ (this is the classical polynomial ambiguity of the entire function [33, 12]).

Remark 3.3 (Interpretation of the kernel and cokernel). If $\mathcal{L}_{\text{TD}}(\Omega)$ were invertible, the Fredholm condition would be vacuous and no adjoint selection would occur. The weight (3.16) is chosen precisely so that this does not happen: the inner counterpart of the shed wake mode is admitted by the downstream weight and furnishes a kernel element, $\dim \ker \mathcal{L}_{\text{TD}}(\Omega) \geq 1$; index zero then forces a cokernel of equal dimension, and (3.19) asserts that no further degeneracy occurs. Physically, the cokernel functional Ψ^* measures resonant forcing of the shed wake mode, and $\langle \mathbf{F}_{KH}, \Psi^* \rangle \neq 0$ states that the wake-mode matching data force their own resonance. The kernel element accounts for the expected inner non-uniqueness: the amplitude of the shed mode is not determined by the inner problem alone but by the matching constraint, which is the content of Theorem 3.7. In the model of Section 4 all of this is explicit.

By the Fredholm alternative, $\text{Ran } \mathcal{L}_{\text{TD}}(\Omega) = \{F \in \mathcal{H}_\sigma : \langle F, \Psi^*(\Omega) \rangle_{\mathcal{H}_\sigma} = 0\}$. Consequently, for the regular forcing in (3.12),

$$\langle \mathbf{F}_{\text{inc}}(\Omega) + A\mathbf{F}_{KH}(\Omega), \Psi^*(\Omega) \rangle_{\mathcal{H}_\sigma} = 0, \quad (3.20)$$

and therefore, provided $\langle \mathbf{F}_{KH}, \Psi^* \rangle \neq 0$, $A_{\text{Fr}}(\Omega) = -\frac{\langle \mathbf{F}_{\text{inc}}(\Omega), \Psi^*(\Omega) \rangle_{\mathcal{H}_\sigma}}{\langle \mathbf{F}_{KH}(\Omega), \Psi^*(\Omega) \rangle_{\mathcal{H}_\sigma}}$.

3.5. Edge singular trace and concomitant

By Lemma 3.1 the matching data decompose as

$$F_{\text{match}}(A) = C_-(A)\mathbf{F}_{\text{sing}} + \mathbf{F}_{\text{reg}}(A), \quad \mathbf{F}_{\text{reg}}(A) = \mathbf{F}_{\text{inc}} + A\mathbf{F}_{KH} \in \mathcal{H}_\sigma,$$

and the singular coefficient is recovered by $\Pi_{\text{sing}} F_{\text{match}}(A) = C_-(A)\mathbf{F}_{\text{sing}}$. The boundary concomitant (3.14), evaluated on a small edge contour ∂B_ρ^+ and paired with the adjoint state, together with the singular trace (3.10) against (b, μ) , defines a finite edge functional $\mathcal{B}_{\text{edge}} : \mathcal{E}_{\text{edge}} \times \ker \mathcal{L}_{\text{TD}}(\Omega)^* \rightarrow \mathbb{C}$ such that

$$\mathcal{B}_{\text{edge}}(G, \Psi^*) = \text{f. p.} \lim_{\rho \downarrow 0} \int_{\partial B_\rho^+} (J^X(G, \Psi^*)n_X + J^Y(G, \Psi^*)n_Y) ds + \text{f. p.} \int_{\mathbb{R}} (g_K^\# b + g_\infty^\# \mu) dX,$$

the second term being the trace-level form used in practice (and in Section 4); see Appendix A. For $G = C r^{-1/2} \mathbf{V}_-$, linearity gives $\mathcal{B}_{\text{edge}}(C r^{-1/2} \mathbf{V}_-, \Psi^*) = C \mathcal{B}_{\text{edge}}(r^{-1/2} \mathbf{V}_-, \Psi^*)$.

Hypothesis 3.4 (Edge-concomitant nondegeneracy). For the adjoint generator in (3.19), $\kappa(\Omega) := \mathcal{B}_{\text{edge}}(r^{-1/2} \mathbf{V}_-, \Psi^*(\Omega)) \neq 0$. Then,

$$\mathcal{B}_{\text{edge}}(C_-(A)r^{-1/2} \mathbf{V}_-, \Psi^*(\Omega)) = C_-(A)\kappa(\Omega). \quad (3.21)$$

The full compatibility relation for data in $\mathcal{D}_{\text{match}} = \mathcal{E}_{\text{edge}} \oplus \mathcal{H}_\sigma$, obtained from the Green identity (A.1) under Hypothesis 3.2(ii), is

$$\mathcal{B}_{\text{edge}}(C_-(A)r^{-1/2} \mathbf{V}_-, \Psi^*) + \langle \mathbf{F}_{\text{inc}} + A\mathbf{F}_{KH}, \Psi^* \rangle_{\mathcal{H}_\sigma} = 0. \quad (3.22)$$

Using (3.21),

$$C_-(A)\kappa(\Omega) + \langle \mathbf{F}_{\text{inc}}(\Omega) + A\mathbf{F}_{KH}(\Omega), \Psi^*(\Omega) \rangle_{\mathcal{H}_\sigma} = 0. \quad (3.23)$$

3.6. Reduction of the Kutta–Fredholm consistency

Relation (3.23) is an identity in A precisely because of the augmented solvability Hypothesis 3.2(ii): the Green pairing holds for the whole affine family, not only for the selected value of A . It therefore determines the adjoint pairing of the regular data a priori in terms of the edge concomitant, which removes the apparent need to impose the consistency relation (1.4) as a separate hypothesis.

Proposition 3.5 (Reduction of the Kutta–Fredholm hypotheses). *Assume Hypothesis 3.2 (both parts) and $\kappa(\Omega) \neq 0$. Then, for every $A \in \mathbb{C}$,*

$$\langle \mathbf{F}_{\text{inc}}(\Omega) + A\mathbf{F}_{KH}(\Omega), \Psi^*(\Omega) \rangle_{\mathcal{H}_\sigma} = -\kappa(\Omega) C_-(A). \quad (3.24)$$

In particular, matching the affine coefficients in A ,

$$\langle \mathbf{F}_{\text{inc}}, \Psi^* \rangle_{\mathcal{H}_\sigma} = -\kappa C_-^{(0)}, \quad \langle \mathbf{F}_{KH}, \Psi^* \rangle_{\mathcal{H}_\sigma} = -\kappa C_-^{(KH)}. \quad (3.25)$$

Consequently:

1. the consistency relation (1.4) holds with $\chi(\Omega) = -\kappa(\Omega) \neq 0$;
2. the nondegeneracy $\langle \mathbf{F}_{KH}, \Psi^* \rangle \neq 0$ holds if and only if $C_-^{(KH)} \neq 0$;
3. the two scalar selection conditions coincide: $C_-(A) = 0 \Leftrightarrow \langle \mathbf{F}_{\text{inc}} + A\mathbf{F}_{KH}, \Psi^* \rangle = 0$.

Thus hypothesis (H4) of Theorem 1.1 is not independent of the others: given the Fredholm realization and the augmented solvability of (H3), it reduces to the single nondegeneracy $\kappa(\Omega) \neq 0$ together with $C_-^{(KH)} \neq 0$ from (H2).

Proof. By Hypothesis 3.2(ii), for each A there is W_A in the augmented class with $\mathcal{L}_{\text{TD}}(\Omega)W_A = F_{\text{match}}(A)$ and a valid Green identity against $\Psi^* \in \ker \mathcal{L}_{\text{TD}}(\Omega)^*$. Since $\mathcal{L}_{\text{TD}}(\Omega)^*\Psi^* = 0$ and the admissible line/decay terms vanish, the only remaining boundary term is the finite edge concomitant, giving (3.22) for that A ; as this holds for every $A \in \mathbb{C}$, substituting (3.21) yields (3.23) identically in A , i.e. (3.24). Because both sides of (3.24) are affine in A and $C_-(A) = C_-^{(0)} + AC_-^{(KH)}$, matching coefficients gives (3.25). Claims (i)–(iii) are immediate: (i) is (3.24); (ii) follows from the second equation in (3.25) and $\kappa \neq 0$; (iii) follows from (3.24) and $\kappa \neq 0$. \square

Remark 3.6. Proposition 3.5 resolves a potential circularity: one need not posit both the regular Fredholm solvability (3.20) and the consistency (1.4) as separate scalar constraints on the single amplitude A . The genuine analytic content is concentrated in (a) the Fredholm realization with augmented solvability, Hypothesis 3.2 (limitation (i) of Section 6 for the true base flow; automatic in the model of Section 4), and (b) the edge-concomitant nondegeneracy $\kappa \neq 0$ of Hypothesis 3.4 (limitation (ii) of Section 6; a theorem in the model, Proposition 4.5). All algebraic results then follow.

3.7. Viscous derivation of $C_-(A) = 0$

The bounded lower-deck class excludes the singular component:

$$W \in \mathcal{X}_\sigma \implies \mathcal{L}_{\text{TD}}(\Omega)W \in \mathcal{H}_\sigma \implies \Pi_{\text{sing}} \mathcal{L}_{\text{TD}}(\Omega)W = 0$$

by Lemma 3.1. Thus a bounded viscous–inviscid matching solution requires

$$\Pi_{\text{sing}} F_{\text{match}}(A) = 0 \iff C_-(A) = 0.$$

Once $C_-(A) = 0$, the remaining forcing lies in \mathcal{H}_σ , and Fredholm solvability is exactly $\langle \mathbf{F}_{\text{inc}} + A\mathbf{F}_{KH}, \Psi^* \rangle_{\mathcal{H}_\sigma} = 0$.

Theorem 3.7 (Kutta selection as Fredholm compatibility). *Assume Hypotheses 3.2 and 3.4 and $C_-^{(KH)} \neq 0$. Then bounded lower-deck matching to the outer family Φ_A^{out} is possible only if $C_-(A) = 0$. Equivalently, $A = A_{\text{Kutta}} = -\frac{C_-^{(0)}}{C_-^{(KH)}}$. For this value of A , the regular lower-deck problem is solvable iff $\langle \mathbf{F}_{\text{inc}}(\Omega) + A_{\text{Kutta}}\mathbf{F}_{KH}(\Omega), \Psi^*(\Omega) \rangle_{\mathcal{H}_\sigma} = 0$. Hence the Kutta-selected and Fredholm-selected amplitudes coincide:*

$$A_{\text{rec}}(\Omega) = A_{\text{Kutta}} = A_{\text{Fr}}(\Omega) = -\frac{\langle \mathbf{F}_{\text{inc}}(\Omega), \Psi^*(\Omega) \rangle_{\mathcal{H}_\sigma}}{\langle \mathbf{F}_{KH}(\Omega), \Psi^*(\Omega) \rangle_{\mathcal{H}_\sigma}}. \quad (3.26)$$

Proof. The matching datum has the decomposition

$$F_{\text{match}}(A) = C_{-}(A)\mathbf{F}_{\text{sing}} + \mathbf{F}_{\text{inc}} + A\mathbf{F}_{KH}, \quad \mathbf{F}_{\text{sing}} \in \mathcal{E}_{\text{edge}}, \quad \mathbf{F}_{\text{inc}} + A\mathbf{F}_{KH} \in \mathcal{H}_{\sigma}.$$

Since $\text{Ran } \mathcal{L}_{\text{TD}}(\Omega) \subset \mathcal{H}_{\sigma}$ and $\mathcal{E}_{\text{edge}} \cap \mathcal{H}_{\sigma} = \{0\}$ (Lemma 3.1), bounded matching implies $C_{-}(A) = 0$. By $C_{-}(A) = C_{-}^{(0)} + AC_{-}^{(KH)}$ and $C_{-}^{(KH)} \neq 0$, $A = -C_{-}^{(0)}/C_{-}^{(KH)}$. For this value the singular part vanishes; by Proposition 3.5 the nondegeneracy $\langle \mathbf{F}_{KH}, \Psi^* \rangle = -\kappa C_{-}^{(KH)} \neq 0$ holds, and the Fredholm alternative gives

$$\mathbf{F}_{\text{inc}} + A\mathbf{F}_{KH} \in \text{Ran } \mathcal{L}_{\text{TD}}(\Omega) \iff \langle \mathbf{F}_{\text{inc}} + A\mathbf{F}_{KH}, \Psi^* \rangle_{\mathcal{H}_{\sigma}} = 0.$$

Solving the scalar equation gives (3.26). The concomitant hypothesis gives the equivalent edge form

$$C_{-}(A) = 0 \iff \mathcal{B}_{\text{edge}}(C_{-}(A)r^{-1/2}\mathbf{V}_{-}, \Psi^*) = 0,$$

because $\kappa(\Omega) \neq 0$. □

Combining the preceding identities, $C_{-}(A) = 0$ iff $\Pi_{\text{sing}} F_{\text{match}}(A) = 0$ iff $\mathbf{F}_{\text{inc}} + A\mathbf{F}_{KH} \in \text{Ran } \mathcal{L}_{\text{TD}}(\Omega)$ and, under Hypothesis 3.2, $\mathbf{F}_{\text{inc}} + A\mathbf{F}_{KH} \in \text{Ran } \mathcal{L}_{\text{TD}}(\Omega)$ iff $\langle \mathbf{F}_{\text{inc}} + A\mathbf{F}_{KH}, \Psi^* \rangle_{\mathcal{H}_{\sigma}} = 0$. Thus the unsteady Kutta condition is the Fredholm compatibility condition of the viscous lower deck, and the selected receptivity amplitude is the adjoint quotient (3.26).

4. Exact verification in the linear-shear lower-deck model

This section verifies the inner hypotheses (H3)–(H4) of Theorem 1.1 in closed form for the canonical linear-shear model of the unsteady lower deck. The model retains exactly the two features on which the selection mechanism rests—the plate/wake switching of the boundary condition at $X = 0$ and the pressure–displacement interaction—while freezing the base flow at its uniform-shear profile. It is the trailing-edge analogue of Terent’ev’s vibrating-ribbon problem [43], and the same model underlies the classical lower-branch receptivity analyses [19, 37]. The result of the section is the following exact instance of Theorem 1.1.

Theorem 4.1 (Exact model selection mechanism). *For the linear-shear lower-deck model (4.2), away from the discrete resonance set Σ of Proposition 4.5, the Kutta amplitude selected by exclusion of the edge singularity coincides with*

the adjoint Fredholm quotient and with the downstream pole residue: $A_{\text{rec}}^{\text{m}}(\Omega) = -\frac{C_{-}^{(0)}}{C_{-}^{(KH)}} = -\frac{\langle \mathbf{F}_{\text{inc}}, \Psi_{\text{m}}^ \rangle_{\mathcal{H}_{\sigma}}}{\langle \mathbf{F}_{KH}, \Psi_{\text{m}}^* \rangle_{\mathcal{H}_{\sigma}}}$ = $i \text{Res}_{\alpha=\alpha_w} \mathcal{M}^{\text{m}}(\alpha; \Omega)$, with $\alpha_w = \Omega^{1/2}$. Moreover the adjoint field is generated mode-wise by the Airy pair*

$$u^*(Y) = \text{Ai}'(z(Y; \alpha)), \quad q(Y) = \frac{c(\alpha)^2}{i\alpha} \text{Ai}(z(Y; \alpha)), \quad (4.1)$$

dual to the primal shear structure $u_Y \propto \text{Ai}(z)$.

Proof. Combine Theorem 4.2 (adjoint structure, giving (4.1)), Proposition 4.4 (Wiener–Hopf reduction, Fredholm structure, and augmented solvability), Proposition 4.5 (nondegeneracy of the edge concomitant, defining Σ), and the general Theorems 3.7 and 5.4; the details occupy Sections 4.2 to 4.4 and are collected in Corollary 4.6. □

4.1. The model operator

Take, in (3.8),

$$U_0 = \lambda_0 Y, \quad V_0 = 0, \quad \lambda_0 > 0, \quad (4.2)$$

with the symmetric-component boundary conditions (3.3), (3.4) and the flat-plate interaction law (3.6). Write $\mathcal{L}_{\text{TD}}^{\text{m}}(\Omega)$ for the resulting operator on the weighted spaces of Section 3.4. The true trailing-edge base state differs from (4.2) by smooth $\mathcal{O}(1)$ terms (displacement, wake centerline acceleration). Throughout, Fourier transforms are $\hat{h}(\alpha) = \int h(X)e^{-i\alpha X} dX$, primal modes are proportional to $e^{i\alpha X}$, adjoint modes to $e^{-i\alpha X}$ (bilinear pairing), and

$$c(\alpha) := (i\alpha\lambda_0)^{1/3}, \quad z(Y; \alpha) := c(\alpha)Y + z_0(\alpha), \quad z_0(\alpha) := -\frac{i\Omega}{c(\alpha)^2}, \quad (4.3)$$

with the principal branch of $(i\alpha\lambda_0)^{1/3}$ cut along $\alpha \in i[0, \infty)$, so that $|\arg c| \leq \pi/6$ for real α and $\text{Ai}(z) \rightarrow 0$ as $Y \rightarrow +\infty$. Also set $\kappa_1(z_0) := \int_{z_0}^{\infty} \text{Ai}(s) ds$, and let $\gamma(\alpha)$ be the analytic continuation of $|\alpha|$ with cuts on the imaginary axis, then $\gamma(\alpha) = |\alpha|$ for $\alpha \in \mathbb{R}$.

4.2. Primal Airy structure, impedances, and the wake pole

For a primal mode $(u, v, p, a) = (f(Y), \hat{v}(Y), \hat{p}, \hat{a})e^{i\alpha X}$, elimination of \hat{v} and \hat{p} by cross-differentiation of (3.8) with (4.2) gives $f''' = (i\alpha\lambda_0 Y - i\Omega)f' = c^2 z f'$, so that f' satisfies the Airy equation in z ; the decaying branch is

$$f'(Y) = B \text{Ai}(z), \quad B \in \mathbb{C}. \quad (4.4)$$

Two half-line impedances follow. *Plate* ($u(0) = v(0) = 0$): integrating (4.4) with $f(0) = 0$ and evaluating the momentum equation at $Y = 0$,

$$i\alpha\hat{p} = f''(0) = Bc \text{Ai}'(z_0), \quad \hat{a} = \frac{B}{c} \kappa_1(z_0), \quad Z_p(\alpha; \Omega) := \frac{\hat{p}}{\hat{a}} = \frac{c^2 \text{Ai}'(z_0)}{i\alpha \kappa_1(z_0)},$$

the classical lower-branch impedance [43, 41]. *Wake* (symmetric: $u_Y(0) = v(0) = 0$): decay of u_Y forces $B = 0$ unless $\text{Ai}(z_0) = 0$; the generic wake mode is therefore the shear-free slug

$$f \equiv \hat{a}, \quad \hat{v} = -i\alpha\hat{a}Y, \quad -i\Omega\hat{a} + i\alpha\hat{p} = 0, \quad (4.5)$$

the convective term $i\alpha\lambda_0 Y \hat{a}$ being cancelled exactly by $\lambda_0 \hat{v}$. Hence

$$Z_w(\alpha; \Omega) := \frac{\hat{p}}{\hat{a}} = \frac{\Omega}{\alpha}. \quad (4.6)$$

Define the plate and wake dispersion functions

$$D_p(\alpha; \Omega) := Z_p(\alpha; \Omega) - \gamma(\alpha), \quad D_w(\alpha; \Omega) := \Omega - \alpha\gamma(\alpha).$$

Zeros of D_p are the lower-branch Tollmien–Schlichting modes of the semi-infinite plate; zeros of D_w are the wake modes of the model. For $\Omega > 0$,

$$D_w(\alpha_w; \Omega) = 0, \quad \alpha_w = \Omega^{1/2} > 0, \quad \partial_\alpha D_w(\alpha_w; \Omega) = -2\Omega^{1/2} \neq 0 : \quad (4.7)$$

a simple, neutral wake pole. Its causal classification follows Briggs–Bers: continuing $\Omega \mapsto \Omega + i\zeta$, $\zeta > 0$, gives $\alpha_w = (\Omega + i\zeta)^{1/2}$ with $\Im\alpha_w > 0$, so the pole descends onto the real axis from above as $\zeta \downarrow 0$ and belongs to the downstream set $\mathcal{P}_{\text{down}}$ of Section 5.3. The symmetric model wake mode is thus the neutral limiting case of the convectively unstable situation $\Im\alpha_{KH} < 0$ of Assumption 2.1; see Remark 4.7 for the antisymmetric (flapping) component.

Introduce the half-line unknowns $\tau(X) := u_Y(X, 0) \mathbf{1}_{X < 0}$, and $U_c(X) := u(X, 0) \mathbf{1}_{X > 0}$, whose transforms $\hat{\tau}_-$, \hat{U}_{c+} are analytic in the upper and lower half-planes respectively. Solving the Y -problem for arbitrary $(\hat{\tau}_-, \hat{U}_{c+})$ and eliminating (\hat{p}, \hat{a}) with the interaction law $\hat{p} = \gamma(\alpha)\hat{a} + \hat{f}_K$ gives the scalar Wiener–Hopf equation

$$D_w(\alpha; \Omega) \hat{U}_{c+}(\alpha) = -\frac{\alpha \kappa_1(z_0)}{c \text{Ai}(z_0)} D_p(\alpha; \Omega) \hat{\tau}_-(\alpha) + \alpha \hat{f}(\alpha), \quad (4.8)$$

where \hat{f} collects the transformed matching data. The kernel is

$$K(\alpha; \Omega) = -\frac{\alpha \kappa_1(z_0(\alpha)) D_p(\alpha; \Omega)}{c(\alpha) \text{Ai}(z_0(\alpha)) D_w(\alpha; \Omega)}, \quad (4.9)$$

meromorphic off the imaginary-axis cuts, with large- α behavior $K = \mathcal{O}(\alpha^{-1/3})$ determined by $z_0 \rightarrow 0$, $D_p \sim -\gamma$, $D_w \sim -\alpha\gamma$; the canonical factorization $K = K_+ K_-$ with zero-free factors exists on any horizontal contour avoiding the zeros of D_p , D_w , $\text{Ai}(z_0)$, and $\kappa_1(z_0)$, with index tracking fixed by the winding number of K along the weighted contour (cf. [32]). The Kutta-normalized response (minimal edge growth; Section 5.1) is the meromorphic function $\mathcal{M}^m(\alpha; \Omega) = \frac{\mathcal{N}^m(\alpha; \Omega)}{D_w(\alpha; \Omega)}$, with \mathcal{N}^m explicit in terms of K_\pm and the data, and the selected wake amplitude of Theorem 5.4 is, by (4.7),

$$A_{\text{rec}}^m(\Omega) = i \text{Res}_{\alpha=\alpha_w} \mathcal{M}^m = -\frac{i \mathcal{N}^m(\Omega^{1/2}; \Omega)}{2 \Omega^{1/2}}. \quad (4.10)$$

4.3. The Airy adjoint

The central computation of this section is that the adjoint system (3.13) is also exactly solvable, with a basis dual to the primal Airy structure.

Theorem 4.2 (Airy structure of the adjoint). *For $U_0 = \lambda_0 Y$, $V_0 = 0$, an adjoint mode $(u^*, q) = (g(Y), \hat{q}(Y))e^{-i\alpha X}$ of (3.13) satisfies the reduced third-order equation*

$$g''' - (i\alpha\lambda_0 Y - i\Omega)g' - 2i\alpha\lambda_0 g = 0, \quad \text{i.e.} \quad g_{zzz} - z g_z - 2g = 0 \quad (4.11)$$

in the variable z of (4.3), and the adjoint pressure is recovered algebraically as

$$\hat{q} = \frac{c^2}{i\alpha} h(z), \quad h := g_{zz} - z g, \quad h_z = g. \quad (4.12)$$

A fundamental system of (4.11) is

$$g \in \text{span}\{Ai'(z), Bi'(z), Gi'(z)\}, \quad (4.13)$$

with companions $h \in \text{span}\{Ai(z), Bi(z), Gi(z)\}$ respectively, where Gi is the Scorer function, $Gi''(z) - z Gi(z) = -1/\pi$ [2]. The solutions admissible as $Y \rightarrow +\infty$ are spanned by the recessive pair and the algebraically decaying Scorer pair,

$$(g, \hat{q}) \in \text{span} \left\{ \left(Ai'(z), \frac{c^2}{i\alpha} Ai(z) \right), \left(Gi'(z), \frac{c^2}{i\alpha} Gi(z) \right) \right\}, \quad (4.14)$$

and the adjoint line states are finite and explicit; in particular, for the recessive component,

$$\bar{U}^*(X) = \int_0^\infty u^* dY = -\frac{Ai(z_0)}{c} e^{-i\alpha X}, \quad \hat{b} \propto i\alpha \frac{Ai(z_0)}{c}. \quad (4.15)$$

Proof. With (4.2) the adjoint system (3.13) reads $-i\Omega u^* - \lambda_0 Y u_X^* - u_{YY}^* - q_X = 0$, $q_Y = \lambda_0 u^*$. Inserting $(g, \hat{q})e^{-i\alpha X}$,

$$-i\Omega g + i\alpha\lambda_0 Y g - g'' + i\alpha\hat{q} = 0, \quad \hat{q}' = \lambda_0 g.$$

Solving the first relation for $i\alpha\hat{q} = g'' + i\Omega g - i\alpha\lambda_0 Y g$ and differentiating, the second relation gives $i\alpha\lambda_0 g = g''' + i\Omega g' - i\alpha\lambda_0 g - i\alpha\lambda_0 Y g'$, which is (4.11); passing to z -units uses $i\alpha\lambda_0 Y - i\Omega = c^2 z$ and $i\alpha\lambda_0 = c^3$. For (4.12), note $i\alpha\hat{q} = c^2 g_{zz} + i\Omega g - (c^2 z + i\Omega)g = c^2(g_{zz} - z g) = c^2 h$, and $h_z = g_{zzz} - g - z g_z = (g_{zzz} - z g_z - 2g) + g = g$ by (4.11). For the basis: if $g = Ai'(z)$ then $g_z = z Ai$, $g_{zz} = Ai + z Ai'$, $g_{zzz} = 2 Ai' + z^2 Ai$, and $g_{zzz} - z g_z - 2g = 2 Ai' + z^2 Ai - z^2 Ai - 2 Ai' = 0$; the same computation holds verbatim for Bi' , and for Gi' using $Gi'' = z Gi - 1/\pi$, the inhomogeneous term cancelling in the combination. The companions follow from $h = g_{zz} - z g$: for $g = Ai'$, $h = Ai''' - z Ai' = (z Ai)' - z Ai' = Ai$, and analogously for the other pairs. Admissibility: $Ai'(z)$ is recessive, $Gi'(z) = \mathcal{O}(z^{-2})$ and $Bi(z) = \mathcal{O}(z^{-1})$ as $z \rightarrow \infty$ in $|\arg z| < \pi/3$ [2], so both (g, \hat{q}) pairs decay, while Bi' grows exponentially and is excluded. Finally $\int_0^\infty Ai'(z) dY = c^{-1}[Ai(z)]_{z_0}^\infty = -c^{-1} Ai(z_0)$, giving (4.15) via $b = \bar{U}_X^*$ from (3.15). \square

Remark 4.3 (Primal–adjoint Airy duality). The primal solution carries its Airy structure in the shear, $u_Y \propto Ai(z)$, with velocity u an Airy integral; the adjoint carries it in the velocity, $u^* \propto Ai'(z)$, with adjoint pressure $q \propto Ai(z)$. This is the lower-deck realization of the familiar duality between direct and adjoint Orr–Sommerfeld structures in receptivity theory [17], here in closed form.

The adjoint half-plane problems mirror the primal ones: on the plate side the condition $u^*(X, 0) = 0$ and on the wake side $u_Y^*(X, 0) = 0$ select one-parameter combinations of the admissible pair (4.14) for each α , and the homogeneous adjoint problem reduces, by the same elimination that led to (4.8), to a scalar Wiener–Hopf problem.

Proposition 4.4 (Wiener–Hopf reduction of the model Fredholm problem). *Let $\Sigma_0(\Omega)$ denote the (closed, discrete in Ω) set of real-contour degeneracies, i.e. those $\Omega > 0$ for which $D_p(\cdot; \Omega)$, $Ai(z_0(\cdot))$, or $\kappa_1(z_0(\cdot))$ vanishes on the weighted inversion contours of Section 3.4. For $\Omega \notin \Sigma_0$ and weights (3.16) with $\vartheta > 0$ sufficiently small:*

1. the frozen (translation-invariant) plate and wake limit operators of $\mathcal{L}_{\text{TD}}^{\text{m}}(\Omega)$ are invertible on their weighted lines, their symbols being governed by D_p and D_w respectively; the adjoint frozen symbols are the transposes and have the same determinants;
2. if the kernel (4.9) admits a canonical factorization $K = K_+K_-$ with zero index along the weighted contour—on which the wake pole α_w lies above the downstream line $\Im\alpha = -\vartheta$ —then $\mathcal{L}_{\text{TD}}^{\text{m}}(\Omega) : \mathcal{X}_\sigma \rightarrow \mathcal{H}_\sigma$ is Fredholm with $\text{ind } \mathcal{L}_{\text{TD}}^{\text{m}}(\Omega) = 0$ and $\dim \ker \mathcal{L}_{\text{TD}}^{\text{m}}(\Omega) = \dim \ker \mathcal{L}_{\text{TD}}^{\text{m}}(\Omega)^* = 1$; the kernel is generated by the inner wake mode $W_w = (e^{i\alpha_w X} \chi_w, \dots)$ built from the slug (4.5), and the cokernel by the adjoint Wiener–Hopf state $\Psi_{\text{m}}^*(\Omega)$ assembled from (4.14);
3. augmented solvability (Hypothesis 3.2(ii)) holds: for every A , the Wiener–Hopf construction with the non-Kutta entire-function normalization produces a solution of $\mathcal{L}_{\text{TD}}^{\text{m}}(\Omega)W_A = F_{\text{match}}(A)$ whose edge behavior realizes the $|X|^{-1/2}$ line trace (3.10), and the Green identity (A.1) holds with finite edge concomitant.

Proof. (i) is the explicit computation of Sections 4.2 and 4.3: the frozen plate (resp. wake) problem is diagonalized by the Fourier transform with symbol determinant proportional to D_p (resp. D_w) after removal of the nonvanishing factors $c \text{Ai}(z_0)$, $\kappa_1(z_0)$; transposition does not change determinants. For (ii), the operator differs from a direct sum of its frozen limits by an interval-supported switching term, so the limit-operator criterion [35] reduces to the invertibility in (i); given the assumed zero-index factorization, the index and the defect dimensions are read off from the standard Wiener–Hopf argument-principle count [32], the downstream weight $\vartheta > 0$ placing α_w on the kernel side of the contour, exactly as in Remark 3.3. For (iii), the entire function $P(\alpha)$ of Section 5.1 may be chosen with one extra polynomial degree; the corresponding solution has the $(|\alpha|^{-3/2})$ edge decay of (5.1), i.e. the $X^{1/2}$ displacement and $|X|^{-1/2}$ trace behavior of $\mathcal{E}_{\text{edge}}$ [33, 12]; the concomitant integrals converge by the explicit local exponents. \square

The factorization condition in (ii) is verified along the real contour for all $\Omega \notin \Sigma_0$, since the kernel (4.9) is then zero-free there and $K = \mathcal{O}(\alpha^{-1/3})$ is compensated by the standard algebraic prefactor; the excluded set is absorbed into the discrete set Σ of Proposition 4.5.

4.4. Nondegeneracy of the edge concomitant

With augmented solvability available, Proposition 3.5 applies unconditionally in the model, and the identity $\langle \mathbf{F}_{KH}, \Psi_{\text{m}}^* \rangle = -\kappa(\Omega) C_{-}^{(KH)}$ converts the nondegeneracy of κ into the computable statement that the wake-mode data are not orthogonal to the adjoint state. The latter pairing is an evaluation at the wake pole and is explicit.

Proposition 4.5 (Model nondegeneracy: (H4) holds off a discrete set). *Let $z_0^w := z_0(\alpha_w)$. Then*

$$z_0^w = \lambda_0^{-2/3} \Omega^{2/3} e^{-5i\pi/6}, \quad (4.16)$$

so that as Ω ranges over $(0, \infty)$ the point z_0^w traverses the fixed ray $\arg z = -5\pi/6$. The wake-mode pairing evaluates, by Parseval, at $\alpha = \alpha_w$:

$$\langle \mathbf{F}_{KH}, \Psi_{\text{m}}^*(\Omega) \rangle_{\mathcal{H}_\sigma} = \frac{C(\Omega)}{K_{-}(\alpha_w; \Omega) \partial_\alpha D_w(\alpha_w; \Omega)} \text{Ai}'(z_0^w), \quad (4.17)$$

where $C(\Omega)$ is a finite product of the normalization constants of ℓ_{KH} , \mathcal{M}_{in} , and the factorization, nonvanishing by construction. Consequently

$$\kappa(\Omega) = -\frac{\langle \mathbf{F}_{KH}, \Psi_{\text{m}}^* \rangle}{C_{-}^{(KH)}} \neq 0 \quad \text{for all } \Omega \in (0, \infty) \setminus \Sigma, \quad (4.18)$$

where $\Sigma \supset \Sigma_0$ is discrete. In particular, under the factorization condition of Proposition 4.4, (H3)–(H4) of Theorem 1.1 hold for the model for all $\Omega \in (0, \infty) \setminus \Sigma$.

Proof. Formula (4.16) is direct: $z_0^w = -i\Omega(i\Omega^{1/2}\lambda_0)^{-2/3} = \Omega^{2/3}\lambda_0^{-2/3}e^{-i\pi/2}e^{-i\pi/3}$. For (4.17): the matching datum \mathbf{F}_{KH} of the (normalized) wake mode is, after the wake-mode subtraction implicit in the weight choice, concentrated on the downstream half-line with profile $\propto e^{i\alpha_w X}$; its bilinear pairing with Ψ_{m}^* is, by Parseval, the evaluation of the adjoint transform at $\alpha = \alpha_w$. The adjoint transform is the Wiener–Hopf solution of Proposition 4.4(ii); at α_w it is a product

of (a) the factor $1/K_-(\alpha_w)$, (b) the simple-zero factor $1/\partial_\alpha D_w(\alpha_w)$ arising from the wake-side elimination, and (c) the recessive adjoint amplitude, which by Theorem 4.2 is proportional to $\text{Ai}'(z_0^w)$; collecting the remaining nonzero normalization constants into $C(\Omega)$ gives (4.17). Nonvanishing: $K_-(\alpha_w) \neq 0$ because the factorization is zero-free by construction; $\partial_\alpha D_w(\alpha_w) = -2\Omega^{1/2} \neq 0$; and $\text{Ai}'(z_0^w) \neq 0$ for every $\Omega > 0$, since all zeros of Ai' lie on the negative real axis [2] while $\arg z_0^w = -5\pi/6 \neq \pm\pi$. The only possible degeneracies are those of $C(\Omega)$ and of the contour conditions defining K_\pm , i.e. zeros of the analytic functions $D_p(\cdot; \Omega)$, $\text{Ai}(z_0(\cdot))$, $\kappa_1(z_0(\cdot))$ on the weighted contours, together with possible zeros of $C_-^{(KH)}$ excluded by (H2); each is the intersection of the zero set of a nontrivial analytic function with a fixed ray or contour, hence a discrete set $\Sigma \subset (0, \infty)$. Combining with Propositions 3.5 and 4.4 yields (4.18) and the final claim. \square

Figure 4 illustrates the proposition numerically: along the wake-pole ray (4.16) the three Airy quantities entering (4.17) and the kernel (4.9) remain bounded away from zero over the sampled frequency range.

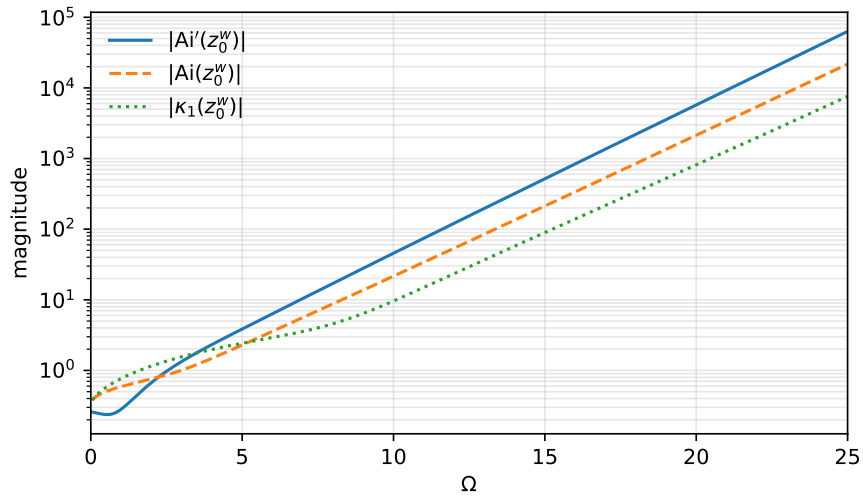


Figure 4: Nondegeneracy along the wake-pole ray (4.16) ($\lambda_0 = 1$): magnitudes of $Ai'(z_0^w)$, $Ai(z_0^w)$, and $\kappa_1(z_0^w)$ for $\Omega \in (0, 25]$. All three factors remain bounded away from zero (sampled minima $\approx 0.24, 0.39$, and 0.38 , respectively), consistent with Proposition 4.5.

Corollary 4.6 (Inner selection in the model). *For the linear-shear model and $\Omega \in (0, \infty) \setminus \Sigma$, the conclusions of Theorem 3.7 hold unconditionally: bounded lower-deck matching enforces $C_-(A) = 0$, the selected amplitude is the adjoint quotient (3.26) with $\Psi^* = \Psi_m^*$ explicit through Theorem 4.2, and it coincides with the wake-pole formula (4.10).*

Remark 4.7 (Antisymmetric component and the genuine KH pole). The computation above is for the symmetric component, whose model wake mode is the neutral slug (4.5). For the antisymmetric (flapping) component, the wake-side conditions (3.5) replace (3.4); the elimination proceeds identically, with (4.6) replaced by the flapping impedance $Z_w^a(\alpha; \Omega)$ obtained from the kinematic condition and the antisymmetric interaction map, and the wake dispersion function $D_w^a = Z_w^a - \gamma^a$ acquires complex zeros with $\Im \alpha_w^a < 0$ (the lower-deck counterpart of the Kelvin–Helmholtz mode), restoring the strict inequality of Assumption 2.1. None of the structural steps changes: the adjoint basis (4.13) is the same (it depends only on the bulk operator), the kernel/cokernel count is the same with $\vartheta > |\Im \alpha_w^a|$, and Proposition 4.5 holds with z_0^w evaluated at α_w^a , the ray (4.16) replaced by a curve in $|\arg z_0^w| < \pi$ still avoiding the negative real axis for $\Im \alpha_w^a < 0$ small. The explicit form of Z_w^a for the true near-wake profile requires the numerical base flow of [22] and is left to future work.

5. Transform representation and pole-residue formula

We connect the Fredholm-selected amplitude of Section 3 with the pole coefficient of the transformed outer problem. Throughout, $\Phi_A^{\text{out}} = \Phi_0^{\text{out}} + A\Phi_{KH}^{\text{out}}$, $C_-(A) = C_-^{(0)} + AC_-^{(KH)}$, and $C_-^{(KH)} \neq 0$. The selected value from the lower deck is $A_{\text{rec}}(\Omega) = -\frac{\langle \mathbf{F}_{\text{inc}}(\Omega), \Psi^*(\Omega) \rangle_{\mathcal{H}_\sigma}}{\langle \mathbf{F}_{KH}(\Omega), \Psi^*(\Omega) \rangle_{\mathcal{H}_\sigma}}$.

5.1. Kutta-normalized Wiener–Hopf representation

For the flat plate, introduce

$$\hat{f}(\alpha) = \int_{-\infty}^{\infty} f(x)e^{-i\alpha x} dx, \quad \hat{f}_+(\alpha) = \int_0^{\infty} f(x)e^{-i\alpha x} dx, \quad \hat{f}_-(\alpha) = \int_{-\infty}^0 f(x)e^{-i\alpha x} dx.$$

With $e^{i\alpha x - i\omega_{\text{phys}} t}$, the $+$ -transform is analytic in a lower half-strip and the $-$ -transform in an upper half-strip. Fourier transformation of

$$\mathcal{L}_{\text{out}} \phi = 0, \quad \mathcal{L}_{\text{out}} = \beta^2 \partial_x^2 + \partial_y^2 + 2iMk_0 \partial_x + k_0^2$$

gives $\partial_y^2 \hat{\phi} - \mu(\alpha)^2 \hat{\phi} = 0$ with $\mu(\alpha)^2 = \beta^2 \alpha^2 + 2Mk_0 \alpha - k_0^2$. The physical branch is fixed by $\Re \mu(\alpha) > 0$ on the inversion contour, with $\alpha_{\pm} = \pm \frac{k_0}{1 \pm M}$ being the acoustic branch points of (2.4). Hence $\hat{\phi}^{\pm}(\alpha, y) = \hat{\phi}^{\pm}(\alpha, 0)e^{\mp \mu(\alpha)y}$ for $\pm y > 0$. The plate condition on $x < 0$ and the sheet condition on $x > 0$ yield a Wiener–Hopf equation [32] of the equation $K(\alpha; \omega_{\text{phys}}, \mathcal{G}) \hat{\eta}_+(\alpha) + \hat{q}_-(\alpha) = \hat{f}(\alpha; \omega_{\text{phys}}, \mathcal{G})$, where K is the scalar kernel obtained from the sheet determinant and \hat{f} is the transformed acoustic forcing. Its zero set contains the spatial wake spectrum:

$$K(\alpha; \omega_{\text{phys}}, \mathcal{G}) = 0 \iff D(\alpha; \omega_{\text{phys}}, \mathcal{G}) = 0 \text{ up to nonzero analytic factors.}$$

Assume a canonical factorization in a common strip \mathfrak{S} : $K(\alpha; \omega_{\text{phys}}, \mathcal{G}) = K_+(\alpha; \omega_{\text{phys}}, \mathcal{G})K_-(\alpha; \omega_{\text{phys}}, \mathcal{G})$, and $K_{\pm}^{\pm 1} \in \mathcal{O}(\mathfrak{S}_{\pm})$ with the retained downstream wake pole excluded from K_-^{-1} and kept explicitly in the meromorphic response.

Splitting $\frac{\hat{f}}{K_-} = \left(\frac{\hat{f}}{K_-} \right)_+ + \left(\frac{\hat{f}}{K_-} \right)_-$ gives $K_+ \hat{\eta}_+ - \left(\frac{\hat{f}}{K_-} \right)_+ = -\frac{\hat{q}_-}{K_-} + \left(\frac{\hat{f}}{K_-} \right)_-$. The two sides extend to an entire function $P(\alpha)$. The edge condition fixes the polynomial ambiguity:

$$C_-(\Phi^{\text{out}}) = 0 \iff P = P_{\text{Kutta}}, \quad (5.1)$$

equivalently, in terms of the Abelian correspondence between the edge behavior of η and the decay of its transform: the non-Kutta state associated with the $r^{1/2}$ potential term has $\eta \sim \text{const} \cdot x^{1/2}$ and hence $\hat{\eta}_+ = O(|\alpha|^{-3/2})$ at infinity in \mathfrak{S}_- , while the Kutta-normalized state has the attached-sheet behavior $\eta \sim \text{const} \cdot x(1 + O(x^{1/2}))$ and hence

$$\hat{\eta}_+(\alpha) = O(|\alpha|^{-2}) \quad (|\alpha| \rightarrow \infty \text{ in } \mathfrak{S}_-),$$

the classification of the edge exponents $x^{1/2}$, x , $x^{3/2}$ being that of Orszag & Crow [33]; see also [12].

Assumption 5.1 (Kutta-normalized meromorphic response). The flat-plate Kutta-normalized outer response has $\hat{\eta}_+(\alpha) = \mathcal{M}(\alpha; \omega_{\text{phys}}, \mathcal{G}) = \frac{\mathcal{N}(\alpha; \omega_{\text{phys}}, \mathcal{G})}{D(\alpha; \omega_{\text{phys}}, \mathcal{G})}$ in the downstream deformation domain \mathfrak{D}_- , where $\mathcal{N}, D \in \mathcal{O}(\mathfrak{D}_-)$ except for acoustic cuts, and

$$D(\alpha_{KH}; \omega_{\text{phys}}, \mathcal{G}) = 0, \quad \partial_\alpha D(\alpha_{KH}; \omega_{\text{phys}}, \mathcal{G}) \neq 0, \quad \mathcal{N}(\alpha_{KH}; \omega_{\text{phys}}, \mathcal{G}) \neq 0.$$

Thus near α_{KH} , $\mathcal{M}(\alpha; \omega_{\text{phys}}, \mathcal{G}) = \frac{\mathcal{R}_{KH}(\omega_{\text{phys}}, \mathcal{G})}{\alpha - \alpha_{KH}} + \mathcal{M}_{\text{hol}}(\alpha; \omega_{\text{phys}}, \mathcal{G})$, where

$$\mathcal{R}_{KH}(\omega_{\text{phys}}, \mathcal{G}) = \text{Res}_{\alpha=\alpha_{KH}} \mathcal{M}(\alpha; \omega_{\text{phys}}, \mathcal{G}) = \frac{\mathcal{N}(\alpha_{KH}; \omega_{\text{phys}}, \mathcal{G})}{\partial_\alpha D(\alpha_{KH}; \omega_{\text{phys}}, \mathcal{G})}.$$

5.2. Uniqueness of the Kutta-normalized outer solution

Let $\mathfrak{K} : \Phi^{\text{out}} \mapsto C_-(\Phi^{\text{out}})$ be the singular edge functional. On the affine outer family, $\mathfrak{K}(\Phi_A^{\text{out}}) = C_-^{(0)} + AC_-^{(KH)}$. Hence

$$A_{\text{Kutta}}^{\text{out}} = -\frac{C_-^{(0)}}{C_-^{(KH)}}. \quad (5.2)$$

Lemma 5.2 (Uniqueness of the Kutta-normalized outer solution). *Assume*

$$\ker \mathcal{A}_{\text{out}}^{\text{hom}} = \text{span}\{\Phi_{KH}^{\text{out}}\}, \quad C_-^{(KH)} \neq 0.$$

Then the set $\{\Phi_{\text{out}}^{\text{out}} : \mathcal{A}_{\text{out}} \Phi_{\text{out}}^{\text{out}} = \mathcal{F}_{\text{out}}^{\text{inc}}, \Phi_{\text{out}}^{\text{out}} \text{ outgoing}, \mathfrak{K}(\Phi_{\text{out}}^{\text{out}}) = 0\}$ contains exactly one element, namely

$$\Phi_{\text{Kutta}}^{\text{out}} = \Phi_0^{\text{out}} - \frac{C_-^{(0)}}{C_-^{(KH)}} \Phi_{KH}^{\text{out}}.$$

Proof. Every outgoing forced solution is Φ_A^{out} . The constraint $\mathfrak{K}(\Phi_A^{\text{out}}) = 0$ is the scalar equation $C_-^{(0)} + AC_-^{(KH)} = 0$, which has the unique solution (5.2). \square

Corollary 5.3 (Identification principle). *If $\tilde{\Phi}^{\text{out}}$ is produced by any transform construction satisfying the same incident field, outgoing convention, and Kutta normalization, then $\tilde{\Phi}^{\text{out}} = \Phi_{\text{Kutta}}^{\text{out}}$. Consequently, its coefficient of Φ_{KH}^{out} is $A_{\text{Kutta}}^{\text{out}}$.*

Combining this with Theorem 3.7,

$$A_{\text{Kutta}}^{\text{out}} = A_{\text{rec}}(\Omega) = -\frac{\langle \mathbf{F}_{\text{inc}}(\Omega), \Psi^*(\Omega) \rangle_{\mathcal{H}_\sigma}}{\langle \mathbf{F}_{KH}(\Omega), \Psi^*(\Omega) \rangle_{\mathcal{H}_\sigma}}. \quad (5.3)$$

5.3. Causal inversion and residue formula for the flat plate

The downstream displacement is recovered by

$$\eta(x) = \frac{1}{2\pi} \int_\Gamma \mathcal{M}(\alpha; \omega_{\text{phys}}, \mathcal{G}) e^{i\alpha x} d\alpha, \quad x > 0. \quad (5.4)$$

The inversion contour Γ is not a free choice; it is fixed by causality. Restore the temporal Laplace by continuing $\omega_{\text{phys}} \rightarrow \omega_{\text{phys}} + i\sigma_t$ with $\sigma_t \rightarrow +\infty$ (the disturbance is switched on at finite time), so that the time transform is analytic in the upper half ω -plane and every spatial pole $\alpha_j(\omega_{\text{phys}} + i\sigma_t)$ is displaced off the real α -axis into a definite half-plane. With the kernel $e^{i\alpha x}$, Γ runs along this causal deformation of the real axis, and the Briggs–Bers classification [5, 4, 31] applies:

$$\alpha_j \in \mathcal{P}_{\text{down}} \iff \Im \alpha_j(\omega_{\text{phys}} + i\sigma_t) > 0 \quad \text{for } \sigma_t \gg 1,$$

with \mathcal{P}_{up} the complementary set. The label is invariant under the continuation $\sigma_t : +\infty \rightarrow 0^+$, even though the pole positions move; $\mathcal{P}_{\text{down}}$ is the causal replacement for the naive orientation-based set. For $x > 0$ the kernel decays in the upper half-plane, so Γ is closed upward and one collects exactly the downstream set:

$$\eta(x) = i \sum_{\alpha_j \in \mathcal{P}_{\text{down}}} \text{Res}_{\alpha=\alpha_j} (\mathcal{M}(\alpha)e^{i\alpha x}) + \eta_{\text{cuts}}(x) + \eta_{\text{arc}}(x), \quad (5.5)$$

the constant $i = \frac{1}{2\pi} \cdot 2\pi i$ being the counterclockwise orientation factor. The Kelvin–Helmholtz pole is critical. At $\sigma_t \gg 1$ it lies in the upper half-plane, hence $\alpha_{KH} \in \mathcal{P}_{\text{down}}$; as $\sigma_t \rightarrow 0^+$ it migrates downward across the real axis to its physical position $\Im\alpha_{KH} < 0$, dragging Γ below it so that the pole remains on the downstream side of the contour. Thus α_{KH} is enclosed by the upward closure despite lying in the lower half-plane: it is a downstream pole that has crossed the axis, which is precisely the statement that the wake mode is an unstable, spatially amplifying disturbance carried into $x > 0$, $e^{i\alpha_{KH}x} = e^{i(\Re\alpha_{KH})x} e^{|\Im\alpha_{KH}|x}$. Its contribution is

$$\eta_{KH}(x) = A_{\text{pole}}(\Omega, \mathcal{G}) e^{i\alpha_{KH}x}, \quad A_{\text{pole}}(\Omega, \mathcal{G}) = i \text{Res}_{\alpha=\alpha_{KH}} \mathcal{M}(\alpha; \omega_{\text{phys}}, \mathcal{G}). \quad (5.6)$$

Since the normalization (2.6) assigns unit displacement amplitude to Φ_{KH}^{out} , $\eta_{KH}(x) = A e^{i\alpha_{KH}x}$ identifies the coefficient of Φ_{KH}^{out} in the inverse-transform solution as $A = A_{\text{pole}}$, with the orientation factor i carried explicitly; no further normalization freedom is invoked. The deformation, and hence (5.6), presupposes convective instability: the descending pole α_{KH} reaches $\Im\alpha_{KH} < 0$ without colliding with a member of \mathcal{P}_{up} . Such a collision is a Briggs–Bers pinch [5, 4], signals the onset of absolute instability, and invalidates the simple downstream residue pickup (the fixed- x response then grows in T and is no longer of the form (5.6)). We assume no pinch throughout; the convective/absolute transition, and any pole–cut collision with the downstream acoustic branch point $\alpha_+ = +k_0/(1 + M)$, are deferred to

Section 6. If α_{KH} is simple, then $A_{\text{pole}}(\Omega, \mathcal{G}) = \frac{i \mathcal{N}(\alpha_{KH}; \omega_{\text{phys}}, \mathcal{G})}{\partial_{\alpha} \mathcal{D}(\alpha_{KH}; \omega_{\text{phys}}, \mathcal{G})}$. Figure 5 shows the the integration contour Γ in the complex α -plane.

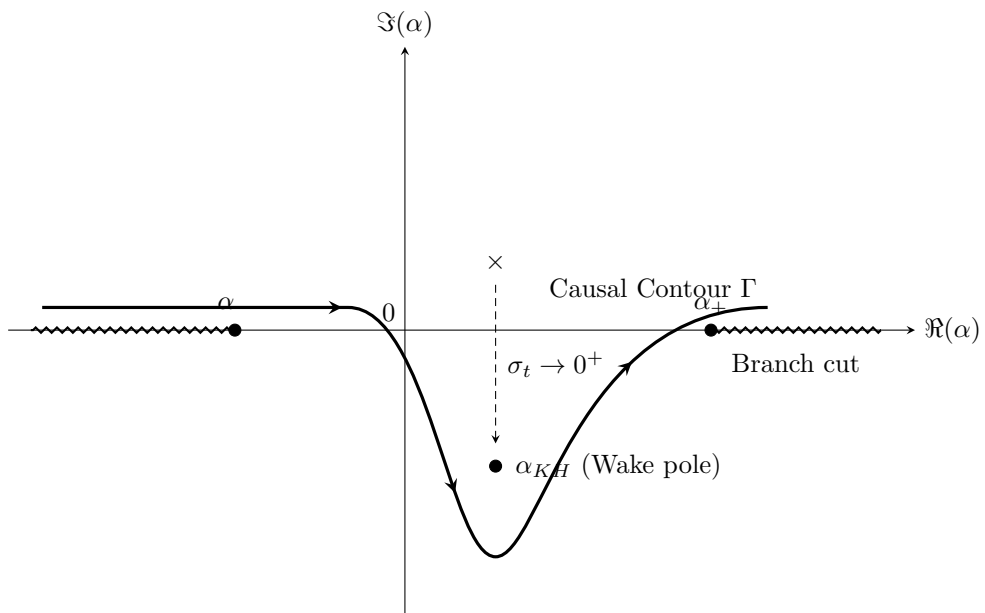


Figure 5: Schematic of the causal integration contour Γ in the complex α -plane. To satisfy causality as $\sigma_t \rightarrow 0^+$, the contour is deformed into the lower half-plane to pass below the moving wake pole α_{KH} . The branch points α_{\pm} and their corresponding branch cuts are also depicted.

Theorem 5.4 (Flat-plate pole-residue formula). *Assume Assumptions 2.1, 5.1, Hypotheses 3.2, 3.4 and $C_-^{(KH)} \neq 0$. Then, with the wake normalization (2.6), $A_{\text{rec}}(\Omega, \mathcal{G}) = -\frac{\langle \mathbf{F}_{\text{inc}}(\Omega), \Psi^*(\Omega) \rangle_{\mathcal{H}_\sigma}}{\langle \mathbf{F}_{KH}(\Omega), \Psi^*(\Omega) \rangle_{\mathcal{H}_\sigma}} = i \text{Res}_{\alpha=\alpha_{KH}} \mathcal{M}(\alpha; \omega_{\text{phys}}, \mathcal{G})$. For a*

$$\text{simple pole, } A_{\text{rec}}(\Omega, \mathcal{G}) = \frac{i \mathcal{N}(\alpha_{KH}; \omega_{\text{phys}}, \mathcal{G})}{\partial_\alpha \mathcal{D}(\alpha_{KH}; \omega_{\text{phys}}, \mathcal{G})}.$$

Proof. By Theorem 3.7, bounded lower-deck matching selects the unique Kutta-normalized outer solution. By Corollary 5.3, the Kutta-normalized Wiener–Hopf solution is the same outer solution. The causal inverse transform (5.4)–(5.6) gives the coefficient of the normalized Φ_{KH}^{out} as $i \text{Res}_{\alpha=\alpha_{KH}} \mathcal{M}$. The adjoint quotient is the same coefficient by (5.3). The simple-pole expression follows from $D(\alpha) = \partial_\alpha \mathcal{D}(\alpha_{KH})(\alpha - \alpha_{KH}) + O((\alpha - \alpha_{KH})^2)$. \square

The formula is invariant under the rescaling

$$\Phi_{KH}^{\text{out}} \mapsto c \Phi_{KH}^{\text{out}}, \quad A \mapsto c^{-1} A,$$

provided the same rescaling is used in \mathbf{F}_{KH} , $C_-^{(KH)}$, and ℓ_{KH} ; the statement above fixes c by (2.6). If

$$D(\alpha_{KH}) = D_\alpha(\alpha_{KH}) = \dots = D_\alpha^{(m-1)}(\alpha_{KH}) = 0, \quad D_\alpha^{(m)}(\alpha_{KH}) \neq 0,$$

then $\mathcal{M}(\alpha) = \sum_{\ell=1}^m \frac{\mathcal{R}_\ell}{(\alpha - \alpha_{KH})^\ell} + \mathcal{M}_{\text{hol}}(\alpha)$, and the downstream contribution is $\eta_{KH}(x) = i e^{i\alpha_{KH}x} \sum_{\ell=1}^m \frac{(ix)^{\ell-1}}{(\ell-1)!} \mathcal{R}_\ell$.

Thus the simple quotient $i\mathcal{N}/D_\alpha$ is valid only when α_{KH} is simple. The geometry derivative of the simple-pole coefficient is

$$\begin{aligned} \partial_\gamma A_{\text{rec}} &= i \frac{\mathcal{N}_\gamma + \mathcal{N}_\alpha \partial_\gamma \alpha_{KH}}{D_\alpha} - i \frac{\mathcal{N}(D_{\alpha\gamma} + D_{\alpha\alpha} \partial_\gamma \alpha_{KH})}{D_\alpha^2}, \\ \partial_\gamma \alpha_{KH} &= -\frac{D_\gamma}{D_\alpha}, \end{aligned}$$

all quantities being evaluated at $(\alpha, \omega_{\text{phys}}, \mathcal{G}) = (\alpha_{KH}, \omega_{\text{phys}}, \mathcal{G})$. Thus, for the flat plate, $A_{\text{rec}} = i \text{Res}_{\alpha=\alpha_{KH}} \mathcal{M}(\alpha; \omega_{\text{phys}}, \mathcal{G})$, and, together with Theorem 3.7,

$$\text{Fredholm lower-deck compatibility} \iff C_-(A) = 0 \iff \text{wake-pole residue selection.} \quad (5.7)$$

The Mellin analogue for finite-angle wedges with self-similar sheet data, including the wedge pole-residue formula (Theorem B.3), is given in Appendix B.

6. Discussion and limitations

We summarize the conditional theory. Let

$$\Phi_A^{\text{out}} = \Phi_0^{\text{out}} + A \Phi_{KH}^{\text{out}}, \quad C_-(A) = C_-^{(0)} + A C_-^{(KH)}, \quad C_-^{(KH)} \neq 0,$$

and assume the simple-pole, edge-indicial, Fredholm (with augmented solvability), edge-concomitant, and Kutta-normalized transform hypotheses:

$$\begin{aligned} D(\alpha_{KH}; \omega_{\text{phys}}, \mathcal{G}) &= 0, \quad D_\alpha(\alpha_{KH}; \omega_{\text{phys}}, \mathcal{G}) \neq 0, \quad \Im \alpha_{KH} < 0, \\ \text{ind } \mathcal{L}_{\text{TD}}(\Omega) &= 0, \quad \ker \mathcal{L}_{\text{TD}}(\Omega)^* = \text{span}\{\Psi^*(\Omega)\}, \quad \kappa(\Omega) = \mathcal{B}_{\text{edge}}(r^{-1/2} \mathbf{V}_-, \Psi^*(\Omega)) \neq 0, \\ \mathcal{M}(\alpha; \omega_{\text{phys}}, \mathcal{G}) &= \frac{\mathcal{N}(\alpha; \omega_{\text{phys}}, \mathcal{G})}{D(\alpha; \omega_{\text{phys}}, \mathcal{G})} \quad \text{near } \alpha_{KH}. \end{aligned}$$

Then the selected amplitude is, with the wake normalization (2.6),

$$A_{\text{rec}}(\Omega, \mathcal{G}) = -\frac{\langle \mathbf{F}_{\text{inc}}(\Omega), \Psi^*(\Omega) \rangle_{\mathcal{H}_\sigma}}{\langle \mathbf{F}_{KH}(\Omega), \Psi^*(\Omega) \rangle_{\mathcal{H}_\sigma}} = -\frac{C_-^{(0)}}{C_-^{(KH)}} = i \text{Res}_{\alpha=\alpha_{KH}} \mathcal{M}(\alpha; \omega_{\text{phys}}, \mathcal{G}).$$

For a simple pole, $A_{\text{rec}}(\Omega, \mathcal{G}) = \frac{i \mathcal{N}(\alpha_{KH}; \omega_{\text{phys}}, \mathcal{G})}{D_\alpha(\alpha_{KH}; \omega_{\text{phys}}, \mathcal{G})}$. Equivalently, $C_-(A) = 0$ iff $\Pi_{\text{sing}} F_{\text{match}}(A) = 0$ iff $\mathbf{F}_{\text{inc}} + A\mathbf{F}_{KH} \in \text{Ran } \mathcal{L}_{\text{TD}}(\Omega)$ iff $\langle \mathbf{F}_{\text{inc}} + A\mathbf{F}_{KH}, \Psi^* \rangle_{\mathcal{H}_\sigma} = 0$. Thus the unsteady Kutta condition is the vanishing of the singular edge trace, not an additional inviscid boundary condition:

$$\text{Tr}_{\text{sing}} \nabla \phi_A^{\text{out}} = C_-(A)r^{-1/2}\mathbf{V}_- = 0 \iff \mathcal{B}_{\text{edge}}(C_-(A)r^{-1/2}\mathbf{V}_-, \Psi^*) = 0.$$

For the linear-shear model of Section 4 the inner hypotheses are theorems (Propositions 4.4 and 4.5), the adjoint state is the Airy-derivative field of Theorem 4.2, and the identities above hold unconditionally for all $\Omega > 0$ outside a discrete resonance set (Corollary 4.6). The distinguished frequency variable is

$$\Omega = Re^{-1/4} \frac{\omega_{\text{phys}} L}{U}, \quad \Omega = O(1) \iff \frac{\omega_{\text{phys}} L}{U} = O(Re^{1/4}).$$

Hence the leading receptivity law has the reduced form $A_{\text{rec}} = A_{\text{rec}}\left(Re^{-1/4} \frac{\omega_{\text{phys}} L}{U}, \mathcal{G}\right)$. For a smooth one-parameter geometry $\mathcal{G} = \mathcal{G}(\gamma)$, the simple-pole sensitivity is

$$\begin{aligned} \partial_\gamma A_{\text{rec}} &= i \frac{\mathcal{N}_\gamma + \mathcal{N}_\alpha \partial_\gamma \alpha_{KH}}{D_\alpha} - i \frac{\mathcal{N}(D_{\alpha\gamma} + D_{\alpha\alpha} \partial_\gamma \alpha_{KH})}{D_\alpha^2}, \\ \partial_\gamma \alpha_{KH} &= -\frac{D_\gamma}{D_\alpha}, \end{aligned}$$

with all functions evaluated at $(\alpha, \omega_{\text{phys}}, \mathcal{G}) = (\alpha_{KH}, \omega_{\text{phys}}, \mathcal{G})$. Thus $\partial_\gamma A_{\text{rec}} = S_{\text{force}} + S_{\text{pole}} + S_{\text{dispersion}}$, where

$$S_{\text{force}} = \frac{i \mathcal{N}_\gamma}{D_\alpha}, \quad S_{\text{pole}} = i \partial_\gamma \alpha_{KH} \left(\frac{\mathcal{N}_\alpha}{D_\alpha} - \frac{\mathcal{N} D_{\alpha\alpha}}{D_\alpha^2} \right), \quad S_{\text{dispersion}} = -\frac{i \mathcal{N} D_{\alpha\gamma}}{D_\alpha^2}.$$

The Mellin analogue for finite-angle wedges with self-similar sheet data is given in Appendix B.

Limitations and extensions

The full trailing-edge base flow introduces three analytic issues that are not settled here. (i) *Fredholm realization*: one must construct weighted spaces for the true unsteady lower-deck operator of [39, 30, 22], prove the index-zero Fredholm property (3.18)–(3.19), and establish the augmented solvability of Hypothesis 3.2(ii); the natural route is the limit-operator decomposition used in Proposition 4.4, with the explicit Airy symbols replaced by the frozen symbols of the numerically known base flow [35]. (ii) *Edge nondegeneracy*: one must prove $\kappa(\Omega) \neq 0$ for the corresponding adjoint state; Proposition 4.5 proves it in the model, where the adjoint is Airy-explicit. (iii) *Spectral degenerations*: multiple wake poles, pole–cut collisions with the acoustic branch points (2.4), Briggs–Bers pinches (the absolute/convective transition, which invalidates the causal downstream pickup of Section 5.3 [5, 4, 31]), and the pole strings generated by non-self-similar wedge sheets [15] all require separate treatment; for a pole of order m the residue formula is replaced by the algebraically growing term $\eta_{KH}(x) = ie^{i\alpha_{KH}x} \sum_{\ell=1}^m \frac{(ix)^{\ell-1}}{(\ell-1)!} \mathcal{R}_\ell$.

A. Formal adjoint and concomitant

Let

$$\Pi = \mathbb{R}_X \times \mathbb{R}_+, \quad \Gamma_p = (-\infty, 0) \times \{0\}, \quad \Gamma_w = (0, \infty) \times \{0\}.$$

The steady lower-deck state satisfies

$$U_{0X} + V_{0Y} = 0, \quad V_0|_{\Gamma_w} = 0.$$

For $W = (u, v, p, a)^\top$, define

$$R_0(W) := u_X + v_Y,$$

$$R_1(W) := -i\Omega u + U_0 u_X + V_0 u_Y + U_{0X} u + U_{0Y} v + p_X - u_{YY}.$$

The primal homogeneous boundary and matching constraints are

$$u = v = 0 \quad \text{on } \Gamma_p, \quad v = 0, \quad u_Y = 0 \quad \text{on } \Gamma_w,$$

$$u(X, Y) - a(X) \rightarrow 0 \quad (Y \rightarrow \infty), \quad p = \mathcal{K}[a].$$

Here $\mathcal{K} = H\partial_X$ such that $\widehat{\mathcal{K}f}(\alpha) = |\alpha|\widehat{f}(\alpha)$. (For the two-sided wake of Section 3.2 the computation below is performed on each half $\pm Y > 0$ and the centerline terms of (3.2) are added; the symmetric component reproduces exactly the formulas of this appendix, and the antisymmetric component differs only in the wake-side boundary block.)

Bulk adjoint

Let $\Psi = (u^*, q)^\top$. Pair $\langle \mathcal{L}_{\text{TD}} W, \Psi \rangle := \iint_{\Pi} \{u^* R_1(W) + q R_0(W)\} dX dY$. Modulo boundary fluxes,

$$\begin{aligned} \iint_{\Pi} u^* U_0 u_X &\equiv - \iint_{\Pi} (U_0 u_X^* + U_{0X} u^*) u, \\ \iint_{\Pi} u^* V_0 u_Y &\equiv - \iint_{\Pi} (V_0 u_Y^* + V_{0Y} u^*) u, \\ \iint_{\Pi} u^* p_X &\equiv - \int_{\mathbb{R}} p \bar{U}_X^* dX, \quad \bar{U}^*(X) := \int_0^\infty u^*(X, Y) dY, \\ - \iint_{\Pi} u^* u_{YY} &\equiv - \iint_{\Pi} u_{YY}^* u, \quad \iint_{\Pi} q u_X \equiv - \iint_{\Pi} q_X u, \\ \iint_{\Pi} q v_Y &\equiv - \iint_{\Pi} q_Y v. \end{aligned}$$

Therefore

$$\begin{aligned} \langle \mathcal{L}_{\text{TD}} W, \Psi \rangle &= \iint_{\Pi} u \left(-i\Omega u^* - U_0 u_X^* - U_{0X} u^* - V_0 u_Y^* - V_{0Y} u^* + U_{0X} u^* - u_{YY}^* - q_X \right) dX dY \\ &\quad + \iint_{\Pi} v (U_{0Y} u^* - q_Y) dX dY - \int_{\mathbb{R}} p \bar{U}_X^* dX + \int_{\partial\Pi} \mathbf{J} \cdot \mathbf{n} ds. \end{aligned}$$

Using $V_{0Y} = -U_{0X}$, this becomes

$$\langle \mathcal{L}_{\text{TD}} W, \Psi \rangle = \iint_{\Pi} u \mathcal{L}_u^* \Psi dX dY + \iint_{\Pi} v \mathcal{L}_v^* \Psi dX dY - \int_{\mathbb{R}} p \bar{U}_X^* dX + \int_{\partial\Pi} \mathbf{J} \cdot \mathbf{n} ds,$$

where

$$\mathcal{L}_u^* \Psi = -i\Omega u^* - U_0 u_X^* - V_0 u_Y^* + U_{0X} u^* - u_{YY}^* - q_X, \quad \mathcal{L}_v^* \Psi = U_{0Y} u^* - q_Y.$$

Hence the formal adjoint equations are

$$-i\Omega u^* - U_0 u_X^* - V_0 u_Y^* + U_{0X} u^* - u_{YY}^* - q_X = 0, \quad q_Y = U_{0Y} u^*.$$

Concomitant

The boundary fluxes are

$$J^X = qu + U_0 u^* u + u^* p, \quad J^Y = qv + V_0 u^* u - (u^* u_Y - u_Y^* u).$$

Equivalently,

$$\mathbf{J} = (J^X, J^Y), \quad J^X = qu + U_0 u^* u + u^* p, \quad J^Y = qv + V_0 u^* u - u^* u_Y + u_Y^* u.$$

The Lagrange identity is

$$u^* R_1(W) + q R_0(W) - u \mathcal{L}_u^* \Psi - v \mathcal{L}_v^* \Psi = \partial_X J^X + \partial_Y J^Y - p \bar{U}_X^* \delta_{Y=\infty},$$

where the last term is understood after integration in Y , equivalently as the line contribution $-\int_{\mathbb{R}} p \bar{U}_X^* dX$.

Adjoint wall and wake conditions

On Γ_p , the primal variations satisfy $u = v = 0$, while u_Y is free. Hence $J^Y|_{\Gamma_p} = -u^*u_Y$, so vanishing of the boundary form for all admissible u_Y gives $u^* = 0$ on Γ_p . On Γ_w , the primal variations satisfy $v = 0$, $u_Y = 0$, and $V_0 = 0$. Hence $J^Y|_{\Gamma_w} = u_Y^*u$, so vanishing for arbitrary admissible u gives $u_Y^* = 0$ on Γ_w . Thus

$$u^* = 0 \quad (X < 0, Y = 0), \quad u_Y^* = 0 \quad (X > 0, Y = 0),$$

with decay conditions chosen so that the fluxes at $X = \pm\infty$ and $Y = \infty$ vanish in the weighted graph norm (with the weights (3.16), adjoint states decay downstream faster than $e^{-\theta X}$).

Adjoint of the interaction and matching constraints

Introduce line multipliers b, μ for

$$p - \mathcal{K}[a] = 0, \quad a - u_\infty = 0, \quad u_\infty(X) := \lim_{Y \rightarrow \infty} u(X, Y).$$

The augmented line pairing is

$$\mathcal{I}_{\text{line}} = - \int_{\mathbb{R}} p \bar{U}_X^* dX + \int_{\mathbb{R}} b(p - \mathcal{K}a) dX + \int_{\mathbb{R}} \mu(a - u_\infty) dX.$$

The coefficient of p gives

$$-\bar{U}_X^* + b = 0 \quad \implies \quad b = \bar{U}_X^*.$$

The coefficient of a gives $\mu - \mathcal{K}^*b = 0$. Since

$$H^* = -H, \quad \partial_X^* = -\partial_X, \quad H\partial_X = \partial_X H,$$

we have $\mathcal{K}^* = (H\partial_X)^* = \partial_X^* H^* = (-\partial_X)(-H) = H\partial_X = \mathcal{K}$. Equivalently, in Fourier variables,

$$\widehat{\mathcal{K}f}(\alpha) = |\alpha| \widehat{f}(\alpha) \quad \implies \quad \mathcal{K}^* = \mathcal{K} \geq 0.$$

Thus $\mu = \mathcal{K}b = \mathcal{K}[\bar{U}_X^*] = H[\bar{U}_{XX}^*]$. The coefficient of u_∞ is $-\mu$, the adjoint far-field traction associated with the displacement matching.

Compact operator form

With

$$\Psi^* = (u^*, q, b, \mu)^\top, \quad \bar{U}^*(X) = \int_0^\infty u^*(X, Y) dY,$$

the formal adjoint of the linearized lower-deck operator is $\mathcal{L}_{\text{TD}}(\Omega)^* \Psi^* = 0$, meaning

$$\begin{cases} -i\Omega u^* - U_0 u_X^* - V_0 u_Y^* + U_0 u^* - u_{YY}^* - q_X = 0, \\ q_Y = U_{0Y} u^*, \\ b = \bar{U}_X^*, \\ \mu = \mathcal{K}[\bar{U}_X^*], \end{cases}$$

with

$$u^* = 0 \quad \text{on } \Gamma_p, \quad u_Y^* = 0 \quad \text{on } \Gamma_w.$$

For admissible W and Ψ^* ,

$$\langle \mathcal{L}_{\text{TD}}(\Omega)W, \Psi^* \rangle_{\mathcal{H}_\sigma} - \langle W, \mathcal{L}_{\text{TD}}(\Omega)^* \Psi^* \rangle_{\mathcal{H}_\sigma} = \int_{\partial\Omega} J(W, \Psi^*) \cdot n ds + \int_{\mathbb{R}} \{b(p - \mathcal{K}a) + \mu(a - u_\infty)\} dX. \quad (\text{A.1})$$

If $W \in \mathcal{D}(\mathcal{L}_{\text{TD}})$ and $\Psi^* \in \mathcal{D}(\mathcal{L}_{\text{TD}}^*)$, all boundary and line terms vanish except possible finite edge contributions.

Finite edge concomitant

Let $B_\rho^+ = \Pi \cap \{X^2 + Y^2 < \rho^2\}$. For a singular edge datum

$$G = C r^{-1/2} \mathbf{V}_-(\theta) \in \mathcal{E}_{\text{edge}}, \quad \mathcal{E}_{\text{edge}} = \text{span}\{r^{-1/2} \mathbf{V}_-\},$$

with lower-deck line traces $(g_\infty^\#, g_K^\#)$ given by (3.10)–(3.11), define

$$\mathcal{B}_{\text{edge}}(G, \Psi^*) := \text{f. p.} \lim_{\rho \downarrow 0} \int_{\partial B_\rho^+} J(G, \Psi^*) \cdot n \, ds + \text{f. p.} \int_{\mathbb{R}} (g_K^\# b + g_\infty^\# \mu) \, dX.$$

The second (trace-pairing) term is the contribution of the pressure–displacement and matching constraints, i.e., the line pairing of (A.1) evaluated on the singular datum; it is the form used in the model computation of Section 4. The finite parts exist because the bulk profile is locally square integrable in two dimensions, the line traces pair against the adjoint line states with local exponents summing above -1 , and the residual divergences are removed by the finite part. Linearity yields $\mathcal{B}_{\text{edge}}(C r^{-1/2} \mathbf{V}_-, \Psi^*) = C \mathcal{B}_{\text{edge}}(r^{-1/2} \mathbf{V}_-, \Psi^*)$. Thus the edge nondegeneracy condition used in the main text is exactly $\kappa(\Omega) := \mathcal{B}_{\text{edge}}(r^{-1/2} \mathbf{V}_-, \Psi^*(\Omega)) \neq 0$. For the outer family, $\mathcal{B}_{\text{edge}}(C_-(A) r^{-1/2} \mathbf{V}_-, \Psi^*(\Omega)) = C_-(A) \kappa(\Omega)$.

Resulting compatibility formula

For decomposed matching data

$$F_{\text{match}}(A) = C_-(A) \mathbf{F}_{\text{sing}} + \mathbf{F}_{\text{inc}} + A \mathbf{F}_{KH}, \quad \mathbf{F}_{\text{sing}} \in \mathcal{E}_{\text{edge}}, \quad \mathbf{F}_{\text{inc}} + A \mathbf{F}_{KH} \in \mathcal{H}_\sigma,$$

the Green identity (A.1), applied under the augmented solvability of Hypothesis 3.2(ii), gives the generalized solvability condition $C_-(A) \kappa(\Omega) + \langle \mathbf{F}_{\text{inc}}(\Omega) + A \mathbf{F}_{KH}(\Omega), \Psi^*(\Omega) \rangle_{\mathcal{H}_\sigma} = 0$. Read as an identity in A (Proposition 3.5), this gives $\langle \mathbf{F}_{\text{inc}} + A \mathbf{F}_{KH}, \Psi^* \rangle_{\mathcal{H}_\sigma} = -\kappa(\Omega) C_-(A)$, hence $\chi = -\kappa$. If the lower-deck solution is required to belong to the bounded graph domain \mathcal{X}_σ , then the singular component is excluded, $\Pi_{\text{sing}} F_{\text{match}}(A) = C_-(A) \mathbf{F}_{\text{sing}} = 0$, and therefore

$$C_-(A) = 0 \text{ iff } \text{Tr}_{\text{sing}} \nabla \phi_A^{\text{out}} = 0 \text{ iff } \langle \mathbf{F}_{\text{inc}} + A \mathbf{F}_{KH}, \Psi^* \rangle_{\mathcal{H}_\sigma} = 0. \text{ Consequently, } A = -\frac{\langle \mathbf{F}_{\text{inc}}(\Omega), \Psi^*(\Omega) \rangle_{\mathcal{H}_\sigma}}{\langle \mathbf{F}_{KH}(\Omega), \Psi^*(\Omega) \rangle_{\mathcal{H}_\sigma}} = -\frac{C_-^{(0)}}{C_{-}^{(KH)}}.$$

B. Mellin analogue for finite-angle wedges

Let the edge be a wedge

$$\Pi_\Theta = \{(r, \theta) : r > 0, -\Theta_- < \theta < \Theta_+\}, \quad \Theta = \Theta_- + \Theta_+.$$

For local wedge fields use the Mellin transform

$$\mathfrak{M}[f](s) = \int_0^\infty r^{s-1} f(r) \, dr, \quad f(r) = \frac{1}{2\pi i} \int_{\Re s = \sigma} r^{-s} \mathfrak{M}[f](s) \, ds.$$

A structural caveat is required which has no flat-plate counterpart. The Mellin transform diagonalizes dilations, not translations; a wake mode that is asymptotically a plane wave $e^{i\alpha x}$ far from the edge is not Mellin-homogeneous, and for general wedge sheets the instability emerges from infinite pole strings $\{s_{KH} - n\}_{n \geq 0}$ generated by the functional-difference structure rather than from a single pole—this is precisely the careful treatment that the instability-wave amplitude requires in [15]. A single-residue statement is therefore meaningful only on the dilation-invariant class:

Assumption B.1 (Self-similar sheet class). The base sheet data in \mathcal{G} are self-similar (sheet strength a pure power of r), so that the homogeneous wake modes of the wedge problem are Mellin-homogeneous, $\eta_{KH} \propto r^{-s_{KH}}$, the wake functional ℓ_{KH} is the coefficient of $r^{-s_{KH}}$, and the Kutta-normalized response (B.2) is meromorphic near a simple wake pole s_{KH} .

The principal separated solutions are

$$\phi(r, \theta) = r^\lambda \Phi_\lambda(\theta), \quad \Phi_\lambda'' + \lambda^2 \Phi_\lambda = 0,$$

or, in Mellin notation, $\lambda = -s$. The wedge walls and sheet conditions produce a finite-dimensional functional-difference system [26, 15]

$$\mathbb{A}(s; \Omega, \mathcal{G})\mathbf{U}(s) + \mathbb{B}(s; \Omega, \mathcal{G})\mathbf{U}(s - 1) = \mathbf{F}(s; \Omega, \mathcal{G}), \quad (\text{B.1})$$

where $\mathbf{U}(s)$ collects Mellin transforms of the angular trace amplitudes and sheet displacement. Its homogeneous determinant is $D_{\text{wedge}}(s; \Omega, \mathcal{G}) := \det \mathbb{T}(s; \Omega, \mathcal{G})$, after reduction of the difference system to a period-one transfer matrix \mathbb{T} . The Kutta-normalized wedge response is assumed meromorphic:

$$\mathcal{M}_{\text{wedge}}(s; \Omega, \mathcal{G}) = \frac{\mathcal{N}_{\text{wedge}}(s; \Omega, \mathcal{G})}{D_{\text{wedge}}(s; \Omega, \mathcal{G})}. \quad (\text{B.2})$$

The wedge faces carry the rigid Neumann conditions $\partial_\theta \phi = 0$ at $\theta = -\Theta_-, \Theta_+$, so the angular pencil $\Phi_\lambda'' + \lambda^2 \Phi_\lambda = 0$ with $\Phi_\lambda'(-\Theta_-) = \Phi_\lambda'(\Theta_+) = 0$ has the Neumann spectrum

$$\lambda_n(\Theta) = \frac{n\pi}{\Theta}, \quad n = 0, 1, 2, \dots, \quad \Theta = \Theta_- + \Theta_+,$$

with eigenfunctions $\Phi_{\lambda_n}(\theta) = \cos\left(\frac{n\pi}{\Theta}(\theta + \Theta_-)\right)$. The first nonconstant root is the loading (pressure-jump) mode

$$\lambda_-(\Theta) = \frac{\pi}{\Theta}, \quad \Psi_-^{(\Theta)}(\theta) = \cos\left(\frac{\pi}{\Theta}(\theta + \Theta_-)\right),$$

which at the cusped/flat-plate value $\Theta = 2\pi$ reduces to $\lambda_- = \frac{1}{2}$ and $\Psi_-^{(\Theta)} = -\sin \frac{\theta}{2}$, recovering Assumption 2.3. The associated velocity singularity is $r^{\lambda_-(\Theta)-1}$, genuinely singular precisely when $\lambda_-(\Theta) < 1$, i.e. $\Theta > \pi$; the admissible trailing-edge range is therefore $\Theta \in (\pi, 2\pi]$, the singularity (and with it the Kutta selection) disappearing as $\Theta \downarrow \pi$. The wedge singular edge-trace space is $\mathcal{E}_{\text{edge}}^{(\Theta)} = \text{span}\{r^{\lambda_-(\Theta)-1}\mathbf{V}_-^{(\Theta)}\}$, replacing $\mathcal{E}_{\text{edge}} = \text{span}\{r^{-1/2}\mathbf{V}_-\}$ in the lower-deck hypotheses. The edge singularity $r^{\lambda_-(\Theta)}\Psi_-^{(\Theta)}(\theta)$ corresponds to a Mellin pole at $s = -\lambda_-(\Theta) = -\frac{\pi}{\Theta}$ under the convention $\mathfrak{M}[r^\lambda] \sim (s + \lambda)^{-1}$. Thus the wedge Kutta normalization is

$$\text{Res}_{s=-\pi/\Theta} \mathcal{M}_{\text{wedge}}(s; \Omega, \mathcal{G}) = 0, \quad C_-(A) = 0,$$

which collapses to $\text{Res}_{s=-1/2} = 0$ only in the cusped limit $\Theta = 2\pi$.

Remark B.2 (Separation of edge and wake poles). For $\mathcal{M}_{\text{wedge}}$ to be well defined near the wake pole s_{KH} , the edge pole and the wake pole must remain distinct, $s_{KH} \neq -\pi/\Theta$: the normalization kills the edge pole and the residue reads off the wake pole. For thin trailing edges $\Theta \rightarrow 2\pi$ this is automatic; as $\Theta \rightarrow \pi^+$ the edge pole $-\pi/\Theta \rightarrow -1$ migrates and may in principle collide with a wake pole.

Let s_{KH} be a simple unstable wake pole:

$$D_{\text{wedge}}(s_{KH}; \Omega, \mathcal{G}) = 0, \quad \partial_s D_{\text{wedge}}(s_{KH}; \Omega, \mathcal{G}) \neq 0. \quad (\text{B.3})$$

Then the inverse Mellin deformation gives

$$\eta(r) = \frac{1}{2\pi i} \int_{\Re s = \sigma} r^{-s} \mathcal{M}_{\text{wedge}}(s; \Omega, \mathcal{G}) ds = \sum_{s_j \in \mathcal{P}} \text{Res}_{s=s_j} (r^{-s} \mathcal{M}_{\text{wedge}}(s)) + \eta_{\text{rem}}(r),$$

the orientation factor being unity here ($\frac{1}{2\pi i} \cdot 2\pi i = 1$, in contrast with the Fourier factor i of (5.5)), and the unstable wedge-mode coefficient is $A_{\text{pole}}^{\text{wedge}}(\Omega, \mathcal{G}) = \text{Res}_{s=s_{KH}} \mathcal{M}_{\text{wedge}}(s; \Omega, \mathcal{G})$. For a simple pole, $A_{\text{pole}}^{\text{wedge}}(\Omega, \mathcal{G}) =$

$$\frac{\mathcal{N}_{\text{wedge}}(s_{KH}; \Omega, \mathcal{G})}{\partial_s D_{\text{wedge}}(s_{KH}; \Omega, \mathcal{G})}.$$

Theorem B.3 (Mellin pole-residue formula). *Assume Assumption B.1, the wedge Mellin representation (B.2), the simple pole condition (B.3), and the lower-deck hypotheses Hypotheses 3.2 and 3.4. Then*

$$A_{\text{rec}}^{\text{wedge}}(\Omega, \mathcal{G}) = -\frac{\langle \mathbf{F}_{\text{inc}}^{\text{wedge}}(\Omega), \Psi_{\text{wedge}}^*(\Omega) \rangle_{\mathcal{H}_\sigma}}{\langle \mathbf{F}_{KH}^{\text{wedge}}(\Omega), \Psi_{\text{wedge}}^*(\Omega) \rangle_{\mathcal{H}_\sigma}} = \text{Res}_{s=s_{KH}} \mathcal{M}_{\text{wedge}}(s; \Omega, \mathcal{G}). \quad (\text{B.4})$$

If s_{KH} is simple, then $A_{\text{rec}}^{\text{wedge}}(\Omega, \mathcal{G}) = \frac{\mathcal{N}_{\text{wedge}}(s_{KH}; \Omega, \mathcal{G})}{\partial_s \mathcal{D}_{\text{wedge}}(s_{KH}; \Omega, \mathcal{G})}$.

Proof. The Mellin transform diagonalizes the radial homogeneity and, under Assumption B.1, converts the wedge trace equations into (B.1) with a Mellin-homogeneous wake mode. Kutta normalization removes the $s = -\pi/\Theta$ edge pole, hence fixes the same one-dimensional kernel as $C_-(A) = 0$. The conditional lower-deck theorem identifies this Kutta-normalized wedge solution with the Fredholm-selected one. The inverse Mellin formula then gives the coefficient of the unstable wedge mode as the residue at $s = s_{KH}$, which yields (B.4); the simple-pole formula follows by the Laurent expansion of $\mathcal{D}_{\text{wedge}}$. \square

Together with Theorem 3.7, the wedge analogue of (5.7) holds verbatim, with $i \text{Res}_{\alpha=\alpha_{KH}} \mathcal{M}$ replaced by $\text{Res}_{s=s_{KH}} \mathcal{M}_{\text{wedge}}$ and the edge space $\mathcal{E}_{\text{edge}}$ by $\mathcal{E}_{\text{edge}}^{(\Theta)}$.

References

- [1] Antoulinakos, F., Wong, P., Jassem, A., Lau, Y., 2018. Absolute instability and transient growth near the band edges of a traveling wave tube. *Physics of Plasmas* 25.
- [2] Apostol, T., Olver, F., Lozier, D., Boisvert, R., Clark, C., 2010. *Nist handbook of mathematical functions*.
- [3] Ayton, L.J., Gill, J.R., Peake, N., 2016. The importance of the unsteady kutta condition when modelling gust–airfoil interaction. *Journal of Sound and Vibration* 378, 28–37.
- [4] Bers, A., 1983. Space-time evolution of plasma instabilities-absolute and convective, in: *Basic plasma physics. 1. volume 1*, pp. 451–517.
- [5] Briggs, R.J., 1964. *Electron-Stream Interaction with Plasmas*. The MIT Press, Cambridge, MA.
- [6] Brown, S., Daniels, P., 1975. On the viscous flow about the trailing edge of a rapidly oscillating plate. *Journal of Fluid Mechanics* 67, 743–761.
- [7] Brown, S., Stewartson, K., 1975. Wake curvature and the kutta condition in laminar flow. *Aeronautical Quarterly* 26, 275–280.
- [8] Cai, J., Chen, X., Gu, L., Chen, J., Chu, N., Wang, L.S., Liang, Y., Yu, J., 2026. Optimal harvesting for nonlinear size-structured populations with nonlocal environmental feedback. *Mathematics* .
- [9] Chen, C.H., Lin, H., Lele, S.K., Santiago, J.G., 2005. Convective and absolute electrokinetic instability with conductivity gradients. *Journal of Fluid Mechanics* 524, 263–303.
- [10] Crighton, D., Leppington, F., 1974. Radiation properties of the semi-infinite vortex sheet: the initial-value problem. *Journal of Fluid Mechanics* 64, 393–414.
- [11] Crighton, D.G., 1972. Radiation properties of the semi-infinite vortex sheet. *Proceedings of the Royal Society of London. A. Mathematical and Physical Sciences* 330, 185–198.
- [12] Crighton, D.G., 1985. The kutta condition in unsteady flow. *Annual Review of Fluid Mechanics* 17, 411–445.
- [13] Daniels, P., 1975. The flow about the trailing edge of a supersonic oscillating airfoil. *Journal of Fluid Mechanics* 72, 541–557.
- [14] Daniels, P., 1978. On the unsteady kutta condition. *The Quarterly Journal of Mechanics and Applied Mathematics* 31, 49–75.
- [15] Davis, A.M., Smith, S.G.L., 2016. Instability of a vortex sheet leaving a right-angled wedge. *Journal of Fluid Mechanics* 803, 1–17.
- [16] Gao, Y., Li, L., Yu, J., 2022. Rolling prediction model of closing price based on eemd data noise reduction and hgs-delm, in: *2022 International Conference on Data Analytics, Computing and Artificial Intelligence (ICDACAI)*, IEEE. pp. 255–260.
- [17] Goldstein, M., Hultgren, L.S., 1989. Boundary-layer receptivity to long-wave free-stream disturbances. *Annual Review of Fluid Mechanics* 21, 137–166.
- [18] Goldstein, M.E., 1983. The evolution of tollmien–schlichting waves near a leading edge. *Journal of Fluid Mechanics* 127, 59–81.
- [19] Goldstein, M.E., 1985. Scattering of acoustic waves into tollmien–schlichting waves by small streamwise variations in surface geometry. *Journal of Fluid Mechanics* 154, 509–529.
- [20] Howe, M.S., 1998. *Acoustics of Fluid-Structure Interactions*. Cambridge University Press, Cambridge, UK.
- [21] Hung, D., Rittersdorf, I., Zhang, P., Chernin, D., Lau, Y., Antonsen Jr, T., Luginsland, J., Simon, D., Gilgenbach, R., 2015. Absolute instability near the band edge of traveling-wave amplifiers. *Physical review letters* 115, 124801.
- [22] Jobe, C.E., Burggraf, O., 1974. The numerical solution of the asymptotic equations of trailing edge flow. *Proceedings of the Royal Society of London. A. Mathematical and Physical Sciences* 340, 91–111.
- [23] Jones, D., Morgan, J., 1972. The instability of a vortex sheet on a subsonic stream under acoustic radiation, in: *Mathematical Proceedings of the Cambridge Philosophical Society*, Cambridge University Press. pp. 465–488.
- [24] King, M.J., Brambley, E.J., Liupekevicius, R., Radia, M., Lafourcade, P., Shah, T.H., 2022. The critical layer in quadratic flow boundary layers over acoustic linings. *Journal of Fluid Mechanics* 950, A8.

- [25] KONDRAT'EV, V.A., 1967. Boundary problems for elliptic equations in domains with conical or angular points. *Trans. Moscow Math. Soc.* 16, 227–313.
- [26] Lawrie, J., King, A., 1994. Exact solution to a class of functional difference equations with application to a moving contact line flow. *European Journal of Applied Mathematics* 5, 141–157.
- [27] Li, X.B., Demange, S., Chen, G., Wang, J.B., Liang, X.F., Schmidt, O.T., Oberleithner, K., 2024. Linear stability and spectral modal decomposition of three-dimensional turbulent wake flow of a generic high-speed train. *Journal of Fluid Mechanics* 1000, A64.
- [28] Liang, Y., Wang, L.S., Yu, J., Liu, Z., 2025. Global well-posedness and stability of nonlocal damage-structured lineage model with feedback and dedifferentiation. *Mathematics* 13, 3583.
- [29] Liu, Z., Wang, L.S., Yu, J., Zhang, J., Martel, E., Li, S., 2025. Bidirectional endothelial feedback drives turing-vascular patterning and drug-resistance niches: a hybrid pde-agent-based study. *Bioengineering* 12, 1097.
- [30] Messiter, A., 1970. Boundary-layer flow near the trailing edge of a flat plate. *SIAM Journal on Applied Mathematics* 18, 241–257.
- [31] Monkewitz, P., 1990. Local and global instabilities in spatially developing flows. *Annual review of fluid mechanics* .
- [32] Noble, B., 1958. *Methods Based on the Wiener-Hopf Technique for the Solution of Partial Differential Equations*. volume 7 of *International Series of Monographs on Pure and Applied Mathematics*. Pergamon Press, New York.
- [33] Orszag, S., Crow, S., 1970. Instability of a vortex sheet leaving a semi-infinite plate. *Studies in Applied Mathematics* 49, 167–181.
- [34] Peake, N., 1994. The viscous interaction between sound waves and the trailing edge of a supersonic splitter plate. *Journal of Fluid Mechanics* 264, 321–342.
- [35] Rabinovich, V., Roch, S., Silbermann, B., 2004. *Limit Operators and Their Applications in Operator Theory*. volume 150 of *Operator Theory: Advances and Applications*. Birkhäuser, Basel.
- [36] Rienstra, S.W., 1981. Sound diffraction at a trailing edge. *Journal of Fluid Mechanics* 108, 443–460.
- [37] Ruban, A., 1984. On the generation of tollmien-schlichting waves by sound. *Fluid Dynamics* 19, 709–717.
- [38] Saric, W.S., Reed, H.L., Kerschen, E.J., 2002. Boundary-layer receptivity to freestream disturbances. *Annual review of fluid mechanics* 34, 291–319.
- [39] Stewartson, K., 1969. On the flow near the trailing edge of a flat plate ii. *Mathematika* 16, 106–121.
- [40] Stewartson, K., 1974. Multistructured boundary layers on flat plates and related bodies. *Advances in Applied Mechanics* 14, 145–239.
- [41] Sychev, V.V., 1998. *Asymptotic Theory of Separated Flows*. Cambridge University Press, Cambridge.
- [42] Taha, H., Rezaei, A.S., 2019. Viscous extension of potential-flow unsteady aerodynamics: the lift frequency response problem. *Journal of Fluid Mechanics* 868, 141–175.
- [43] Terent'Ev, E., 1981. The linear problem of a vibrator in a subsonic boundary layer. *Journal of Applied Mathematics and Mechanics* 45, 791–795.
- [44] Wang, L.S., Yu, J., 2025. Analysis framework for stochastic predator–prey model with demographic noise. *Results in Applied Mathematics* 27, 100621.
- [45] Wang, L.S., Yu, J., 2026. Algebraic–spectral thresholds and discrete–continuous stability transfer in leslie–gower systems. *Electronic Research Archive* 34, 251–290.
- [46] Wang, L.S., Yu, J., Li, S., Liu, Z., 2025a. Analysis and mean-field limit of a hybrid pde-abm modeling angiogenesis-regulated resistance evolution. *Mathematics* 13, 2898.
- [47] Wang, L.S., Yu, J., Liang, Y., Zhang, J., 2026a. The breakdown of linear quasi-cycles: Demographic noise and absorbing boundaries in finite predator–prey systems. *Electronic Research Archive* 34, 4248–4289.
- [48] Wang, L.S., Yu, J., Liang, Y., Zhang, J., 2026b. Elliptic criticality versus volta memory in indirect chemotaxis cascades. *Transport Phenomena* 1, 20260061.
- [49] Wang, L.S., Yu, J., Liu, Z., 2026c. A damage-structured pde model of stem cell hierarchies: The dual role of dedifferentiation in tissue homeostasis and aging. *Plos one* 21, e0335163.
- [50] Wang, Z., Wang, D., Yu, J., 2025b. Multi-strategy hybrid improved intelligent algorithm for solving uav-mtsp. *Information Technology and Control* 54, 413–438.
- [51] Wu, X., 2001. On local boundary-layer receptivity to vortical disturbances in the free stream. *Journal of Fluid Mechanics* 449, 373–393.
- [52] Xia, X., Mohseni, K., 2017. Unsteady aerodynamics and vortex-sheet formation of a two-dimensional airfoil. *Journal of Fluid Mechanics* 830, 439–478.
- [53] Xie, Y., Zhu, Z., Xie, L., Wang, R., Li, S., Zhang, G., Du, Q., Zhu, J., 2025. Local and global instability of the rotating-disk boundary layer of a rotor-stator cavity. *Journal of Fluid Mechanics* 1021, A35.
- [54] Yu, J., Wang, L.S., 2026. Beyond diagonal noise: A better predator-prey modeling framework with cross-covariance. *PLoS One* 21, e0350127.
- [55] Yu, J., Wang, L.S., Ban, S., Liang, Y., 2026a. From microscopic damage to macroscopic games: a dimensionality reduction of stem cell homeostasis. *Transport Phenomena* 1, 20260037.
- [56] Yu, J., Wang, L.S., Liang, Y., 2026b. Rigorous analysis of a nonlocal transport–renewal system for physiologically structured populations. *Mathematical Methods in the Applied Sciences* .
- [57] Yu, J., Wang, L.S., Liu, Z., Liu, J., 2026c. Pattern suppression and recovery under one-way versus two-way chemotactic coupling in hybrid partial differential equation–ordinary differential equation models. *Transport Phenomena* .
- [58] Zhong, X., Wang, X., 2012. Direct numerical simulation on the receptivity, instability, and transition of hypersonic boundary layers. *Annual Review of Fluid Mechanics* 44, 527–561.
- [59] Zhu, W., McCrink, M.H., Bons, J.P., Gregory, J.W., 2020. The unsteady kutta condition on an airfoil in a surging flow. *Journal of Fluid Mechanics* 893, R2.
- [60] Zuccher, S., Luchini, P., 2014. Boundary-layer receptivity to external disturbances using multiple scales. *Meccanica* 49, 441–467.